

# HYDROCLIMATIC VARIABILITY IN THE DWANGWA RIVER BASIN: ASSESSMENT OF LARGE-SCALE FORCING IMPACTS.

# MASTER OF SCIENCE IN ENVIRONMENTAL SCIENCE

By

# AUBREN CHADENENEKA CHIRWA

**Bachelor of Education, University of Malawi** 

Submitted in partial fulfilment of the requirements for the Degree of Master of Science in Environmental Science

**UNIVERSITY OF MALAWI** 

#### **ABSTRACT**

The influence of the El Niño Southern Oscillation (ENSO) and Indian Ocean Dipole (IOD) persists as one of the drivers of climate variability worldwide. There are numerous studies on their evolution, triggering mechanisms, life cycles, and periodicities relating them to the local climate. This study was aimed at assessing the impact of ENSO and IOD on climate variability and river discharge in the Dwangwa Basin. It further assessed climate variability and the response of river discharge in relation to ENSO and IOD between 1985 and 2015. The direction and significance of trends in the rainfall data series were investigated using the non-parametric Mann-Kendall test. The influence of ENSO and IOD was checked by correlating the October-January Nino 3.4 and IOD. Twenty-three years (1985–2008) of river discharge data were classified using Sea Surface Temperature (SST) anomaly data from the equatorial Pacific and Indian Ocean as occurring during an El Niño (warm event), La Nina (Cold event), Positive IOD (warm), and Negative IOD (cold). Correlations and responses were achieved using Pearson product moment and linear regression, respectively. The study found an insignificant (0.05%) negative trend annually in rainfall in the basin. Moreover, rainfall was negatively correlated with El Niño and positive IOD, though insignificant. The river is associated with a decrease in discharge during El Niño and Positive IOD. The opposite was noted during the cold (La Niña) and neutral phase. Study suggests that Dwangwa River Basin experience low rainfall when the SST are warmer in Pacific and Indian Ocean.

# **DECLARATION**

I, the undersigned, hereby declare that this thesis is my own original work which has not been submitted to any other university or institution for similar purposes. Where other people's work has been used, acknowledgements have been made.

Aubren Chadeneneka Chirwa

Signature

# CERTIFICATE OF APPROVAL

The undersigned certify that this thesis represents the student's own work and effort and has been submitted with our approval.

Coordinator, Master of Science in Environmental Science

# **DEDICATION**

I dedicate this work to my wife, Edda Kondwani Chirwa, and to my daughter, Chanju Chirwa. I pass on my sincere gratitude to my beloved family for giving me encouragement and hope. May the mighty living God bless them. It is my innermost wish that my child will draw inspiration from this as she pursues her individual academic efforts.

#### **ACKNOWLEDGEMENTS**

I would like to thank the living God, who sustains us by his grace. My special thanks and foremost appreciation go to my Supervisor, Professor C. Ngongondo, whose consistent encouragement saw me through my studies and whose valuable contributions helped to build the thesis. I acknowledge with high regard his unwavering availability for my cause and his guidance throughout the research project. Special thanks should also go to the Coordinator of the Programme, Associate Professor E. Vunain for supporting me in this study.

My appreciation also goes to the Head teacher of Kawale Community Day Secondary School, Mr. J. Kunchenga, and the entire staff. Special thanks should go to the Ministry of Irrigation and Water Development in Malawi for the assistance rendered in providing discharge data.

I am also grateful to Mr. Chavula (retired), the agro-meteorologist from the Department of Climate Change and Meteorological Services, for providing rainfall data. Many thanks should go to Mr. J. Nyengere, Mr. G. Namasika, Miss. E. Mkandawire, and Mr. P. Chizala for guiding me in statistical areas.

Many thanks also to my brothers and sisters Collins Chirwa, Edith Chirwa, Danwood M. Chirwa (Prof), Christina Chirwa, Giliad Chirwa, Vincent Chirwa (late), Nelson Chirwa, Wadson Chirwa (Jnr.), and Kumbukani Chirwa.

# TABLE OF CONTENT

ABST	TRACT	.iv
TABI	LE OF CONTENT	.ix
LIST	OF TABLES	xiii
LIST	OF FIGURES	xiv
CHAI	PTER ONE	2
INTR	ODUCTION	2
1.1	Background	2
1.2	Problem statement	4
1.3	Objectives of the study	6
1.3.1	Main Objective	6
1.3.2	Specific Objectives	6
1.3.3	Assumptions of the study	6
1.3.4	Hypothesis	7
1.4	Justification of the study	8
1.5	Organisation of the Thesis	8
CHAI	PTER TWO	9
LITE	RATURE REVIEW	9
INTR	ODUCTION	9
2.1	El Niño Southern-Oscillation (ENSO)	9

2.1.1	ENSO influence on rainfall	10
2.2	Indian Ocean Dipole	12
2.2.1	Influence of IOD on rainfall	14
2.3	Rainfall trends	16
2.4	River Discharge Response	19
CHAI	PTER THREE	23
METI	HODOLOGY	23
3.1	Research Design	23
3.2	Study Area	23
3.3	Data Collection	24
3.3.1	Rainfall data	24
3.3.2	River discharge data	25
3.3.3	El Niño Southern Oscillation data	27
3.3.4	SST Anomalies	28
3.3.5	Indian Ocean Dipole data	28
3.4	Data Analysis	30
3.4.1	Quality Control and Statistical Homogeneity Testing	30
3.4.2	Test for Outliers	30
3.4.3	Test for Homogenisation	32
3.4.4	Test for randomness and persistence	34
3.4.5	Temporal trend analysis	35

3.4.6	Rainfall and Areal Mean Characteristics	37			
3.5	River discharge response to ENSO and IOD				
3.6	Correlation analysis of rainfall and SST				
CHAI	PTER FOUR	41			
4.0	RESULTS AND DISCUSSIONS	41			
4.1.	Rainfall variability	41			
4.2	Discharge characteristics	42			
4.3	Rainfall data Validation	43			
4.3.1	Outlier detection	43			
4.3.2	Homogenisation test	43			
4.3.3	Autocorrelation Analysis of Annual and Monthly Series	44			
4.4	Temporal Trend Analysis	45			
4.4.1	Annual and monthly rainfall series trend	45			
4.4.2	Areal mean monthly and annual total trend	47			
4.5	Mean Annual River Discharge	48			
4.6	Correlation between SST and Rainfall in Dwangwa River Basin	49			
4.6.1	ENSO with rainfall and areal mean	50			
4.7	Correlation between Dipole Mode Index (DMI) and rainfall	51			
4.8	River discharge response to ENSO and IOD	52			
4.9	Discussion of results	56			
491	Climate variability in Dwanowa River Basin	56			

4.9.2	Climate trend in Dwangwa River Basin	58
4.9.3	Impact of ENSO and IOD on Rainfall in Dwangwa River Basin	58
СНАРТ	ER FIVE	62
5.0 CO	ONCLUSION AND RECOMMENDATIONS	62
REFER	ENCES	ii
APPEN	DICES	12
APPE	ENDIX A. Homogenisation tests	12
APPE	ENDIX C. ANOVA for river discharge data	4

# LIST OF TABLES

Table 1 Active stations and co-ordinates in Dwangwa Basin	25
Table 2 of PCI, CV and annual mean of the rainfall stations	42
Table 3 Grubbs test for Outliers/Two tailed test	43
Table 4 Homogeneity tests using Pettitt's, Buishand and SNHT	43
Table 5 Summary of Monthly Mann Kendall test for Mwimba station	45
Table 6 Summary of Mann Kendall test for Kaluluma station	46
Table 7 Summary of Mann Kendall test for Kasungu	46
Table 8 Summary of Mann Kendall test for Dwangwa station	47
Table 9 Summary of Mann Kendall trend tests for Areal Mean monthly and annual	
total trend	48
Table 10 Correlation between Rainfall and Nino 3.4 during El Niño Years	50
Table 11 Correlation between Rainfall and Nino 3.4 during La Niña Years	51
Table 12 Correlation between Rainfall and Nino 3.4 during Neutral phase	51
Table 13 Correlation between Rainfall and DMI during Positive IOD	51
Table 14 Correlation between Rainfall and DMI during Negative IOD	52
Table 15 Correlation between Rainfall and DMI during Neutral Phase	52

# LIST OF FIGURES

Figure 1 Schematic diagram showing the wind direction during PIOD13
Figure 2 Schematic diagram showing the wind direction during NIOD
Figure 3 Dwangwa River Basin, showing rivers, stations and gauging stations24
Figure 4 Nino 3.4 Anomaly showing years of El Niño, La Niña and Neutral Phase28
Figure 5 Indian Ocean Dipole Mode Anomaly29
Figure 6 Mean monthly discharge of Dwangwa River Basin (1985-2009)42
Figure 8 Mean Annual Discharge at S53
Figure 9 a. and b. are Regression of Kwengwere and Dwangwa Road Bridge S53 by Nino 3.4
during El Niño
Figure 10 a. and b. are Regression of Kwengwere and Dwangwa Road Bridge S53 by Nino
3.4 during La Niña
Figure 11 a. and b. are Regression of Kwengwere and Dwangwa Road Bridge S53 by Nino
3.4 during Neutral Phase 54
Figure 12 a. and b. are Regression of Kwengwere and Dwangwa Road Bridge S53 by IOD+
54
Figure 13 a. and b. are Regression of Kwengwere and Dwangwa Road Bridge S53 by
Negative IOD55
Figure 14 a. and b. are Regression of Kwengwere and Dwangwa Road Bridge S53 by Nino
3.4 during Neutral Phase
Figure 15 (a) Pettitt test (b) SNHT (c) Buishand Homogenisation tests graphs for Kasungu
station
Figure 16 Homogeneity Test a, b, c and d
Figure 17 (a) ANOVA of S53 (b) Model Parameters (S53)

Figure 18 Regression graph of S53 by Kwengwere	Figure	18 Regression	graph of S53 by	Kwengwere5	,
--	--------	---------------	-----------------	------------	---

#### ACCRONYMS AND ABBREVIATIONS

ANOVA Analysis of Variance

AR Annual Rainfall

CAB Congo Air Boundary

COADS Comprehensive Ocean Atmosphere Data Set

CV Coefficient Variation

DRB Dwangwa River Basin

DRC Democratic Republic of Congo

DWASCO Dwangwa Sugar Corporation

ENSO El Niño Southern Oscillation

ESD Extreme Studentised Deviate

ETp Potential Evapotranspiration

FAO Food and Agriculture Organisation

GOM Government of Malawi

IO Indian Ocean

IOD Indian Ocean Dipole

IODM Indian Ocean Dipole Mode

IODZM Indian Ocean Dipole Mode/Zone Mode

IPCC Intergovernmental Panel on Climate Change

ITCZ Inter-tropical Convergence Zone

MASH Multiple Analysis of Series for Homogenisation

MK Mann-Kendall Test

NOAA National Oceanic and Atmospheric Administration

NWRMP National Water Resources Master Plan

PCI Precipitation Concentration Index

PDO Pacific Decadal Oscillation

PNA Pacific North America

QBO Quasi Biennial Oscillation

SADC -FANR Southern Africa Development Community-Food Agriculture

SLP Sea Level Pressure

SNHT Standard Normal Homogenisation Test

SOI Southern Oscillation Index

SST Sea Surface Temperature

SST Sea Surface Temperature

SSTA Sea Surface Temperature Anomaly

SW South Western

UNDP United Nations Development Programmes

WMO World Meteorological Organisation

WP West Pacific

WRA Water Resources Authority

#### **CHAPTER ONE**

#### INTRODUCTION

# 1.1 Background

Previously, El Niño Southern Oscillation (ENSO) received greater attention as the most significant sea surface temperature (SST) anomaly, exerting enormous force in modulating climate in many parts of the world (Ibebuchi, 2023; Jiang et al., 2021; Nash, 2017). However, studies have become more prevalent since the discovery of IOD as one of the most important SSTs, almost in equal terms with ENSO (Amirudin et al., 2020; Ngongondo et al., 2020; Zhang et al. 2022). Amirudin et al. (2020) presented IOD as being equally important in modifying rainfall, almost in the same manner as ENSO in Southeast Asia. Similarly, Zhang et al. (2022) demonstrated that both IOD and ENSO could be drivers of anticyclonic circulation across the western North Pacific (WNP) throughout the summer in Eastern China. The studies display that the phenomena is important in driving climate systems of the region.

However, in most southern African literature, ENSO has received more attention than IOD ((Jury, 2013; Kambombe et al., 2021; Kumbuyo et al., 2015). Although IOD is not regarded as powerful as ENSO in the climate regime in Southern Africa, Manatsa et al. (2008) found that the influence of IOD on summer rainfall in Zimbabwe is overwhelming compared with that of ENSO when the two are in competition. The IOD influence remains high (significant above the 99% confidence level) even after the

influence of ENSO has been removed, while that of ENSO collapses to insignificance (even at a 90% confidence level) when the IOD contribution is removed.

Yet there are country-based studies that have explicitly examined IOD at the same time as ENSO, and the effects on the temporal-spatial climate variability in southern Africa are relatively small (e.g., Manatsa et al. 2008). Similarly, in Malawi, studies that have looked at the implications of both ENSO and IOD are scarce (Kumbuyo et al. 2015; Ngongondo et al. 2023). Yet, droughts in Central and Southern Malawi have been linked with El Niño (Pauw et al. 2010; Jury, 2013). Recent studies by Kambombe et al. (2021) found contrary results: not every El Niño event leads to low rainfall in some areas in the southern region of Malawi, such as areas in the Lake Chilwa basin. In this case, it is agreeable that ENSO falls short of completely accounting for sub-regional rainfall variability (Manatsa et al. 2008).

Nevertheless, Thulu et al. (2017) presented the northern part of Malawi as being connected with increases in rainfall during the El Niño season. While the central and southern regions displayed a decrease in rainfall during the event. However, studies that looked at both phenomena in the country, such as Kumbuyo et al. (2015) revealed that summer rainfall in Malawi had a strong and significant correlation with the Indian Ocean SST compared to the Atlantic and Pacific Ocean SSTs while using the Pearson correlation coefficient method. The study showed that it is the Indian Ocean Dipole (IOD), not ENSO that has a greater link with rainfall in the country.

The most recent studies, though, by Ngongondo et al. (2020), employed a multivariate framework of statistical models to examine the contributions of low-frequency climate

variability indicators in Lake Malawi, such as the Indian Ocean Dipole Mode (IODM) and the Nino Southern Oscillation (ENSO), and hydro-climate forcing factors, such as rainfall, lake evaporation, and inflowing discharge. The study found the evaporation of open water to have a greater influence on rainfall than covariates such as IOD and ENSO. This shows that local climatic conditions would be of greater importance in understanding the role global circulations play in influencing local climates.

This necessitates extensive research involving additional smaller drainage basins within Lake Malawi. The Dwangwa River Basin is one of the inputs to the water balance of the Lake Malawi basin. This study expands on earlier efforts to understand important global forces in the basin. Thus, the present study advances most previous studies in Malawi, which mainly looked at larger spatial stretches of the country. This study analyses the hydroclimatic variability and examines the larger-scale forcing impacts of ENSO and IOD on the hydrological regime of the Dwangwa River Basin.

#### 1.2 Problem statement

Despite ENSO forming a key component of many seasonal forecasting systems in Southern Africa, both Lizcano and Todd (2005) and Manatsa et al. (2008) insist that most dry and wet regional rainfall anomalies are determined by the Indian Ocean Dipole Mode Index (IODM) and Atlantic Ocean teleconnections rather than the remote Pacific ENSO. The IOD is argued to have similar east-west anomalies, periodicities, and magnitudes in the Indian Ocean (IO), which are generally comparable to those produced by strong ENSO events in the Pacific (Kug et al. 2020). It was also found that the impact of the Indian Ocean Dipole/Zonal Mode Index (IODZMI) is far greater than that of

ENSO on East African rainfall (Saji and Yamagata, 2003). Positive IOD events, rather than El Niño, dominated the enhancement of East African rainfall (Jiang et al., 2021).

Other studies suggest that East Africa shares a maritime rainfall regime with the West Indian Ocean (IO), whereas convection over southern Africa is inversely related (Manatsa et al. 2008). Despite the availability of profound studies on global circulation in southern Africa relating to regional rainfall, few studies have specifically examined Malawi. Studies targeting the local basins in the country remain scarce. Among the few local studies of Malawi, Jury and Mwafulirwa (2002) found a clear correlation between the Malawi Rainfall Index and ENSO. However, the literature on how individual local catchments are affected by this phenomenon remains narrow. Moreover, diverse findings are being presented in recent literature on the impact of ENSO on the hydrological responses of watersheds.

Kambombe et al. (2021) indicated that not every El Niño event leads to low rainfall in the Lake Chilwa Basin. In fact, the study indicated some notable increases in rainfall events in the stations of Chanco, Makoka, Naminjiwa, and Zomba RTC. Interestingly, Thulu et al. (2017) displayed that the northern part of Malawi is connected with increases in rainfall during the El Niño season. While the central and southern regions displayed a decrease in rainfall during the El Niño season, Sceptical, though, is the gap in the literature that has specifically looked at the regions lying in the transition zones, such as the Dwangwa River Basin. Therefore, this gap has prompted this study to assess the impact of ENSO and IOD on the climate variability and discharge response of the Dwangwa River. Importantly, the Dwangwa River is one of the key inflows into Lake Malawi. From an environmental perspective, any changes in the hydrological regime

of the basin can affect the ecological functioning of both the Lake Malawi Basin and the Dwangwa River Basin.

## 1.3 Objectives of the study

## 1.3.1 Main Objective

The main objective of this study is to examine the impact of ENSO and IOD on climate variability and discharge of Dwangwa River Basin.

## 1.3.2 Specific Objectives

- (a) To evaluate the perceived and observed evidence of climate variability in Dwangwa River Basin.
- (b) To assess the impact of ENSO and IOD on the rainfall regime of Dwangwa River Basin.
- (c) To examine the response of discharge of Dwangwa River Basin during ENSO and IOD events.

## 1.3.3 Assumptions of the study

This study is based on the following assumptions. First, there was no climate variability in the Dwangwa Basin, as pointed out by other authors (for example, Ngongondo et al. 2011). Additionally, it is assumed that ENSO and IOD impact the country differently, because the nation lies in the transition zone of ENSO (Jury and Mwafulirwa, 2002). Finally, it is assumed that rainfall has an impact on water discharge; hence, the impact exerted on global circulation will also have an impact on the discharge response.

# 1.3.4 Hypothesis

- $H_o$ : ENSO and IOD have no impact on climate variability and River discharge in Dwangwa Basin.
- $H_a$ : ENSO and IOD have an impact on climate variability and river discharge in Dwangwa Basin.

## 1.4 Justification of the study

ENSO and IOD are natural phenomena that play a great role in influencing rainfall in different regions of the world (Ibebuchi, 2023). They have their own return periods with different signatures in the climates of different regions. Thus, this study endeavours to provide additional insights for future studies. Moreover, better characterisation of local hydro-climatic patterns will enhance the understanding of global atmospheric dynamics and influence stream flow and precipitation. More significantly, on the lower course of the basin, there is a delta with a large swamp where sugar estate plantations are dependent on the Dwangwa River for irrigation. The river is one of the major rivers that form the inflow of the Lake Malawi water balance (Kumambala, 2010).

This means that additional available studies will enable environmentalists to have accurate, long-term rainfall and streamflow forecasting in relation to global circulation, which is vital for effective water resource management. Meanwhile, multi-purpose water resource projects rely heavily on running rivers, and rainfall is currently being threatened by global circulation (IPCC, 2006). Therefore, studies related to climate change are pertinent for the proper utilisation and management of water resources.

## 1.5 Organisation of the Thesis

The dissertation is structured as follows: Chapter one gives the background of this study. Chapter two reviews the literature that has examined this topic, guided by the main and specific objectives. Chapter three presents the methodology adopted to answer the hypotheses adopted in this study. Chapter four presents the result and provides an analysis and interpretation of the findings. Chapter five concludes and provides recommendations based on the findings of this study.

#### **CHAPTER TWO**

#### LITERATURE REVIEW

#### **INTRODUCTION**

This section draws on some of the literature on related studies. This is crucial for identifying the fundamental variables used in this study. This study outlines the ENSO, IOD, and other rainfall-bearing systems in Malawi. In the first part, it is concerned with defining the global circulations (the Indian Ocean Dipole and El Niño Southern Oscillation) as independent variables, yet rainfall and river discharge as dependent variables.

## 2.1 El Niño Southern-Oscillation (ENSO)

The El Niño Southern Oscillation (ENSO) refers to a series of clear and sometimes very strong variations in the sea surface temperature (SST), convective rainfall, surface pressure, and atmospheric circulation through the equatorial Pacific Ocean (Salau et al. 2015). In ordinary situations, the SST in the east of the Southern Pacific Ocean is lower than that in the west of the Southern Pacific Ocean (Kug et al. 2020). Thus, a high-pressure zone dominates the east of the Southern Pacific Ocean. The difference between high- and low-pressure engineers is the blowing of trade winds or easterlies from east to west in the Pacific Ocean (Kug et al. 2020). Therefore, in the equatorial region, trade winds influence the movement of warm surface water from east to west.

However, the opposite occurred during the El Niño period; the SST in the west was lower than that in the east of the southern Pacific Ocean. This large-scale pressure oscillation in the Pacific Ocean is called the Southern Oscillation (SO) (Kug et al. 2020). Consequently, the direction of the trade winds changes, and the warm ocean current move from west to east. The temperatures on the coast of Peru and Southern Ecuador became warmer, signalling El Niño. The two phenomena, El Niño and Southern Oscillation, are known as the ENSO (Kug et al. 2020). It usually peaks around Christmas, hence, the name of the phenomenon. El Niño is Spanish for Christ Child. La Niña refers to the cold equivalent of El Niño (Kug et al. 2020).

#### 2.1.1 ENSO influence on rainfall

Currently, different parts of the world have seen pace in studies of ENSO and some climatic parameters, such as temperature, rainfall, and discharge (Kane, 2009; Sahu et al. 2012; Isla et al. 2013; Salau et al., 2016; Roy, 2017). ENSO varies in the way it modulates the climate in different areas. Salehizadeh et al. (2015) evaluated the effects of large-scale climate factors, such as ENSO, on the occurrence and severity of seasonal precipitation parameters in the Fasa region of Iran using the Pearson correlation technique and other statistical tests. It was discovered that the Southern Oscillation Index (SOI) correlation yielded the highest ENSO effect on Fasa's precipitation in Iran, with a concurrent reverse of as much as 99% in December, December, and October with a one-month lag of 99% and in October with a 3-month lag of 95%.

Many studies have shown that El Niño and La Niña have opposing effects on climate variability in different areas. Pui et al. (2011) reported that ENSO remains the leading driver of rainfall variability over eastern Australia, particularly further inland during

the winter and spring seasons. In Pakistan, Rashid (2004) found negative effects of El Niño on summer monsoon (July–September) rainfall. Similarly, Susilo et al. (2013) showed that El Niño events have a stronger effect on rainfall than La Niña events in Central Kalimantan, Indonesia. Similarly, in Southern Africa, earlier studies by Mason and Tyson (1992) found an association between warmer SST (El Niño) across the West Indian Ocean and rainfall deficits over the region. In contrast, Lee (2015) found that rainfall in the Southern Sumatra and Southern Java Islands, which face the Indian Ocean, is positively correlated with La Niña. In south-western Nigeria, Nnawuike (2016) showed that ENSO events have no significant relationship with rainfall amounts at any of the stations in the region.

Interestingly, in the same country, Salau et al. (2016) investigated the effects of ENSO on temperature and rainfall and reported that a minor northward (southward) shift in the mean position of the Inter-Tropical Convergence Zone (ITCZ) during La Niña (El Niño) events is followed by a reduction (increase) in the average temperature within Nigeria, while the mean precipitation increases (decreases) over the country. This confirms that the ENSO influence is different worldwide. Other areas experienced increased rainfall during La Niña; the opposite occurred during El Niño; and the opposite was observed in other areas.

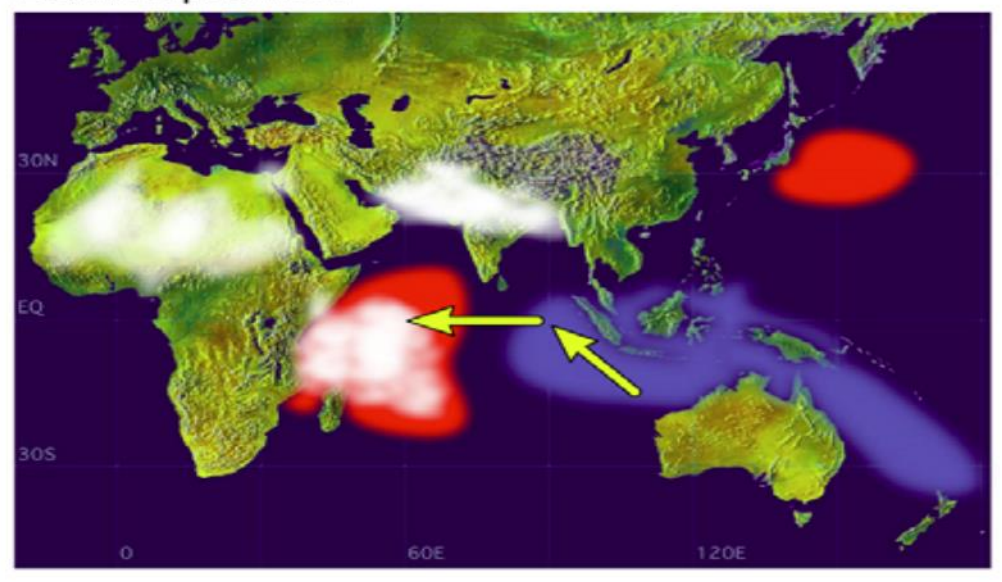
In Malawi, a few studies (e.g., Mwafulirwa, Kumbuyo et al. 2014) have shown that global circulation exerts a substantial impact on water resources, such as flooding and severe droughts. It is pointed out by Jury and Mwafulirwa (2002) and Kumbuyo et al. (2014) that climate change studies to date have largely focused on biophysical aspects, with attention given to the impact of crop yield and livestock production. Jury and Mwafulirwa (2002) and Kumbuyo et al. (2014), using spectral analysis of the rainfall index, revealed cycles at 3.8 years, 2.4 years, and 11.1 years, suggesting links with ENSO, quasi-biennial oscillation (QBO), and the solar cycles, respectively.

A positive correlation between rainfall in Malawi and Ethiopia was reported by Nkhokwe (1996), who found associations between the Southern Oscillation Index (SOI) and the Stratospheric Quasi-Biennial Oscillation (QBO), a change in the zone wind in the equatorial stratosphere from easterly to westerly over a period of approximately 28 months. Goddard and Graham (1999) found that northern Malawi lies near the transition zone of ENSO influence, with opposing centres of action in southern and eastern Africa. However, the literature on the impact of global circulations on local catchment areas remains inadequate at all-time scales.

# 2.2 Indian Ocean Dipole

The Indian Ocean Dipole is a coupled ocean-atmosphere climate mode in the tropical Indian Ocean. During a positive IOD event, SST is anomalously warm in the western Indian Ocean and colder than normal in the east, as shown in Figures 1 and 2 (Saji et al. 1999; Hrudya et al. 2021). SST anomalies are shaded (red shows warm anomalies and blue shows cold anomalies).

## Positive Dipole Mode

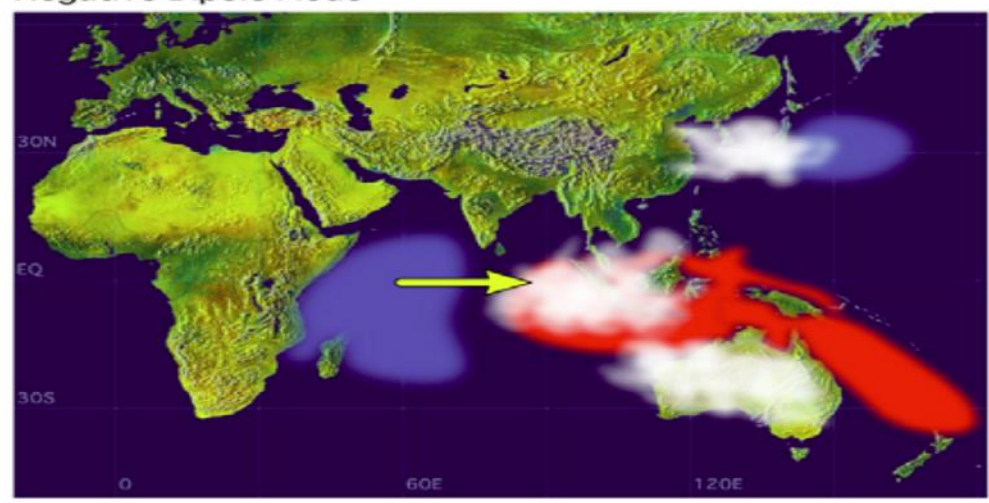


White cloudy patches indicate increased convective activity, and Yellow arrows indicate anomoulous wind directions during Positive IOD events

Figure 1 Schematic diagram showing the wind direction during PIOD

**Source:** http://www.jamstec.go.jp/frsgc/research/dI//iod

#### Negative Dipole Mode



White cloudy patches indicate increased convective activity, and Yellow arrows indicate anomoulous wind directions during Negative IOD events

Figure 2 Schematic diagram showing the wind direction during NIOD

The Indian Ocean Dipole Mode (IODM) is another important manifestation of tropical air-sea interactions (Behera et al. 2005; Yamagata et al. 2003; Hrudya et al. 2021). It has similar east-west anomalies and periodicities and has magnitudes in the Indian Ocean (IO), which are generally comparable to those produced by strong ENSO events in the Pacific. This phenomenon is known to act independently of ENSO, although at times it comes in phase with ENSO events (Manatsa et al. 2008).

#### 2.2.1 Influence of IOD on rainfall

The Indian Ocean Dipole Mode (IODM) is another important manifestation of tropical air-sea interactions (Behera et al. 2005; Yamagata et al. 2003; Hrudya et al. 2021). It has similar east-west anomalies and periodicities and has magnitudes in the Indian Ocean (IO), which are generally comparable to those produced by strong ENSO events in the Pacific. This phenomenon is known to act independently of ENSO, although at times it comes in phase with ENSO events (Manatsa et al. 2008).

Various studies have attempted to link the influence of ENSO and the Indian Ocean Dipole in modifying local climates. For example, earlier studies by Behera et al. (2005) noted that the Indian Ocean Dipole has an overwhelming influence on the East African short rains (October to December) compared to that of the ENSO. However, recent studies by Hoell et al. (2017) showed that the IOD complements the ENSO-related atmospheric response over Southern Africa by strengthening the regional equivalent barotropic Rossby Wave, anomalous mid-tropospheric vertical motions, and anomalous precipitation.

The argument stems from the earlier findings of Saji and Yamagata (2003), who used partial correction analysis to show that positive IOD events dominate the enhancement of East African rainfall rather than El Niño. Additionally, Pui et al. (2012) found that the combined impacts of ENSO and IOD are fairly spatially homogeneous in Australia, with stronger impacts in the inland east and southeast regions, respectively. However, the influence of the IOD, similar to ENSO, varies within the same region. Contemporary studies in Australia by Pepler et al. (2014) reported that IOD has a strong influence on zonal wind flow during the winter and spring months, with positive IOD increasing both onshore winds and rainfall over the coastal strip while decreasing rainfall elsewhere in southeast Australia. The study concludes that IOD opposes the influence of ENSO over the coastal strip, and this is the primary cause of the breakdown of the ENSO-rainfall relationship in the region.

Other studies have been conducted linking IOD with rainfall in different parts of the world, but none of them came up with a single result. It is noted that in other areas, a negative IOD contributes to increased rainfall; however, in other areas, it is associated with droughts. For instance, Ashok et al. (2001) found that a positive Indian Ocean Dipole Mode Index (IODMI) leads to droughts over the Indonesian region and heavy rains and floods over East Africa. Similarly, Lee (2015) showed that rainfall in southern Sumatra and the Southern Java Islands is positively correlated with negative IOD, while in northwestern Sumatra, it is positively correlated with positive IOD.

Mason and Tyson (1999) concluded that East Africa shares maritime rainfall with the West Indian Ocean, while convection over Southern Africa is inversely related. The IOD has been categorised as a major ocean-atmosphere-coupled phenomenon in the tropical Indo-Pacific Sector (Saji et al. 1999).

Investigations into the variability of Africa's climate and, in particular, the probable links between rainfall and SST in neighbouring oceanic areas are increasing in number (e.g., Behara and Yamagata, 2001). Similarly, much of this interest is being stirred by the vulnerability of Southern Africa to large-scale flooding and drought events (Reason and Jagadheesha, 2005). However, the literature on the impact of IOD on the rainfall regime of Malawi remains scarce. It is believed that the occurrence of rainfall around the world is influenced by several large-scale climatic modes. Therefore, it is imperative to study the impact of neighbouring oceanic influences on local climatic regimes.

## 2.3 Rainfall trends

Different factors are believed to have contributed significantly to recent climatic anomalies worldwide. Many parts of the world are witnessing seasonal and inter-annual variability in rainfall. Rainfall is one of the most important climatic parameters that greatly influences droughts and floods (Coscarelli and Caloiero, 2012). Studies on the temporal and spatial characteristics of rainfall have been conducted extensively worldwide (Zhang et al. 2008). Bibi et al. (2014) showed that there is a decreasing trend in the months after the inception of rainfall and an increasing trend in rainfall amounts and frequency towards the middle of the wet season, especially in the northern part of Nigeria.

Earlier studies by Rhodhe and Virji (1976) analysed the trends and periodicity of annual rainfall over East Africa. Spectral analysis of the time series revealed major peaks centred at 2–2.5, 3.5, and 5.6 years. Fauchereau et al. (2003) found substantial disparities in precipitation in Southern Africa, especially in decades. Dry periods have become longer and more intense in Southern Africa, and it is reported by the Intergovernmental Panel on Climate Change (IPCC) that there was an increasing precipitation amount from 1901 to 2005 from the equator to tropical eastern Africa and a decreasing trend in Africa south of 20 °S latitude.

Studies of rainfall characteristics in Malawi include those by Jury and Mwafulirwa (2002), Mbano et al. (2008), and Kumbuyo et al. (2010). Studies by Ngongondo et al. (2011), which examined 42 stations in the country excluding Lake Malawi from 1960 to 2006, revealed statistically non-significant decreasing rainfall patterns for annual, seasonal, monthly, and individual months from March to December. Furthermore, it was found that January and February were the months with the highest rainfall; however, they had overall positive but statistically non-significant trends countrywide, suggesting a higher concentration of seasonal rainfall around these months.

Furthermore, Ngongondo et al. (2011) found an increase in the interannual rainfall variability in Malawi. Similarly, Kumbuyo et al. (2014) found a strong inter-annual fluctuation in rainfall, with topography and location playing major roles in annual rainfall distribution. Spectral analysis of the rainfall time series revealed cycles of five—eight years, suggesting links with the El Niño Southern Oscillation and double the period of the Quasi Biennial Oscillation (QBO) (Kumbuyo et al. 2014). Apart from the

common cycles, the study further pointed out that the rainfall time series of the two zones showed periods of 13.64 and 10.06 years, respectively, which suggests links with the solar cycles that are unswerving with those found in other South African countries.

Earlier studies by Jury and Mwafulirwa (2002) found similar cycles in their study of climate variability in Malawi. Additionally, Nicholson et al. (2013) revealed two surprising features of the rainfall regimes. One was a region with a strong rainfall maximum in the austral autumn along the western shore of Lake Malawi. Second, there was a brief period of reduced rainfall in mid-February that appeared to signal a shift in the prevailing rainfall and circulation regime in the country. The prevailing atmospheric circulation was markedly different before and after the break, as were the characteristics of the rainy season.

Vincent et al. (2014) show that the inter-annual variability in the wet season rainfall in Malawi is influenced by the Indian Ocean Sea Surface Temperature (SST), which varies from year to year, mainly due to the El Niño Southern Oscillation (ENSO) phenomenon. However, it is noted that the influence of ENSO on the climate of Malawi may be difficult to predict as Malawi is located between two regions of opposing climatic responses to El Niño. Eastern equatorial Africa tends to receive above-average rainfall in El Niño conditions, while south-eastern Africa often experiences below-average rainfall, and the opposite response pattern occurs during La Niña conditions (Vincent et al. 2014).

The rainy season extends from November to March, is initially intermittent, and becomes more continuous in January. The ITCZ is predominantly oceanic, and its

position changes with the warmest sea surface temperatures (SSTs) (Marchant et al. 2007). It is thus affected by variations in both the Pacific and Indian Oceans, which in turn are affected by the ocean-atmosphere phenomena of the El Niño Southern Oscillation (ENSO) and Indian Ocean Dipole (IOD), respectively (Tierney et al. 2008).

# 2.4 River Discharge Response

Due to persistent changes in climate, hydrological regimes respond differently to such considerations. Since early civilisation, water in rivers has been crucial for the survival of people. However, owing to changes in climate and anthropogenic activities, river floods cause massive social, economic, and environmental damage and loss of life in many parts of the world (Zhang et al. 2006).

Many studies in different parts of the world have linked floods and droughts to ENSO (Ward et al. 2010; Isla et al. 2013; Babatolu and Akinnubi, 2014; Roudier et al. 2014). Zubair (2001) studied the relationship between ENSO and the Mahaweli River discharge in Sri Lanka and found that El Niño contributed to a decrease in river discharge from January to September. Similarly, Zhang et al. (2006) investigated the variability and possible teleconnections between the annual maximum stream flow from the lower, middle, and upper Yangtze River basins and the El Niño/Southern Oscillation ENSO. The study found different phase relationships between the annual maximum stream flow of the Yangtze River and ENSO in the lower, middle, and upper Yangtze River Basins.

Ouyang et al. (2014) investigated the single and combined impacts of ENSO and Pacific Decadal Oscillation (PDO) on precipitation and stream flow in China over the last

century. The results indicate that precipitation and streamflow decrease during El Niño/PDO warm phase periods and increase during La Niña/PDO cool phase periods in the majority of China, although there are regional and seasonal differences. Schimdt et al. (2001) examined the influence of the ENSO on seasonal rainfall and river discharge in Florida. Seasonal precipitation and streamflow both exhibited strong responses to ENSO. Casimiro et al. (2011) assessed the impact of ENSO on hydrology in Peru. It was found that during strong El Niño years, sharp increases occurred in the discharges in the north-central area of the Pacific coast and decreased in the remaining discharge stations.

During the years classified as La Niña, positive changes were mostly observed in the majority of the stations in the rivers located in the centre of the Pacific Coast of Peru. Another important result of this work is that the Ilave River (south of the Titicaca watershed) shows higher positive (negative) impacts during La Niña (El Niño) years, a fact that is not clearly seen in the rivers of the northern part of the Titicaca watershed (Ramis and Huancane rivers). In contrast, Sahu et al. (2012) examined the impact of ENSO on the Paranaiba Catchment in Brazil and found that extremely high streamflow events were exceptionally associated with canonical Niño Modoki years.

In Canada, Gobena and Gan (2006) investigated the impacts of the El Niño Southern Oscillation, Pacific-North America (PNA) pattern, West Pacific (WP) pattern, and Pacific Decadal Oscillation (PDO) teleconnections on inter-annual to inter-decadal variability of Southwestern (SW) Canadian stream anomalies. The results show that El Niño (La Niña) episodes lead to significant negative (positive) streamflow anomalies in several sub-regions during the spring and summer months following the ENSO onset

year. Studies in Africa on the interannual changeability of river flow remain obscure (Servat et al. 1998). Studies by Jury and Mwafulirwa (2002) analysed annual streamflow for the Blue and White Nile, Congo, Niger, Senegal, Zambezi, and Orange rivers and inflow to Lake Malawi. The study found that the hydrological anomalies in Africa and adjacent South America were sensitive to coupling between zonal circulations over the tropical Atlantic, the global ENSO phase, and the Atlantic Dipole.

Alemaw and Chaoka (2006) examined the variability of annual river runoff and its possible association with the 1950–1998 seasonal El Niño Southern Oscillation in 502 rivers gauged in nine countries in Southern Africa. It was found that there is a possible link between surface water resources in terms of the mean annual runoff and warm ENSO events. This shows that El Niño contributes to an increase in the discharge of most rivers in southern Africa. In Malawi, ongoing research specifically targeting local catchment areas in relation to global circulation and streamflow trends remains narrow. Available studies in the country, e.g., Thulu et al. (2017) examined rainfall trends for El Niño Seasons over Malawi from 1970 to 2016 and their implication on crop yield and hydropower generation.

The study displayed the opposite impact that the phenomenon exerts in Malawi. Earlier, Jury (2013) studied the climatic drivers of Malawi's Shire River, using direct measurements and model estimates to analyse the annual and decadal variability, and concluded that global climate patterns related to wet years include a Pacific La Niña cool phase and low pressure over northeastern Africa. Shire river floods coincide with a cyclonic looping wind pattern that amplifies the equatorial trough and draws a monsoon flow from Tanzania.

Kachaje et al. (2016) studied the potential impact of climate change on hydropower: an assessment of the Lujeri micro hydropower scheme using the Mann Kendall test and found that temperatures have increased significantly in the basin, which might affect river discharge. With this little literature on the impact of teleconnections targeting local catchment areas, the aim of this study is to contribute to ongoing efforts on the topic in Malawi.

#### **CHAPTER THREE**

#### **METHODOLOGY**

## 3.1 Research Design

According to Creswell (2014), cited in Asenahabi (2019), research design is the overall plan for connecting the conceptual research problems to pertinent and achievable empirical research. In this regard, the study used a quantitative research design. The design was adopted because the study used secondary data for SST, rainfall, and gauging station data. In order to trace the relationship that exists between the SST and hydro-climatic variables, the study predominantly used a correlational design. It is a type of non-experimental design that examines the relationship between two or more variables (Asenahabi, 2019). Regression analysis was adopted to check the response of discharge in relation to the changes in the SST.

# 3.2 Study Area

The study was conducted in the Dwangwa River Basin (DRB), which covers a catchment area of 7768 km2 before it drains into Lake Malawi Kumambala (2010). It has a mean annual rainfall of 902 mm and an annual runoff of 12%. The basin is labelled as Water Resources Unit (WRA) 6 according to the National Water Resources Master Plan (NWRMP) (Kumambala, 2010). The basin is located in the central region of Malawi at a height between 500 and 1500 m above mean sea level (Kumambala, 2010). The upper course of the basin in the east and central parts comprises the Kasungu plain,

which is gently undulating with altitudes between 975 and 1300 m above sea level (Kumambala, 2010).

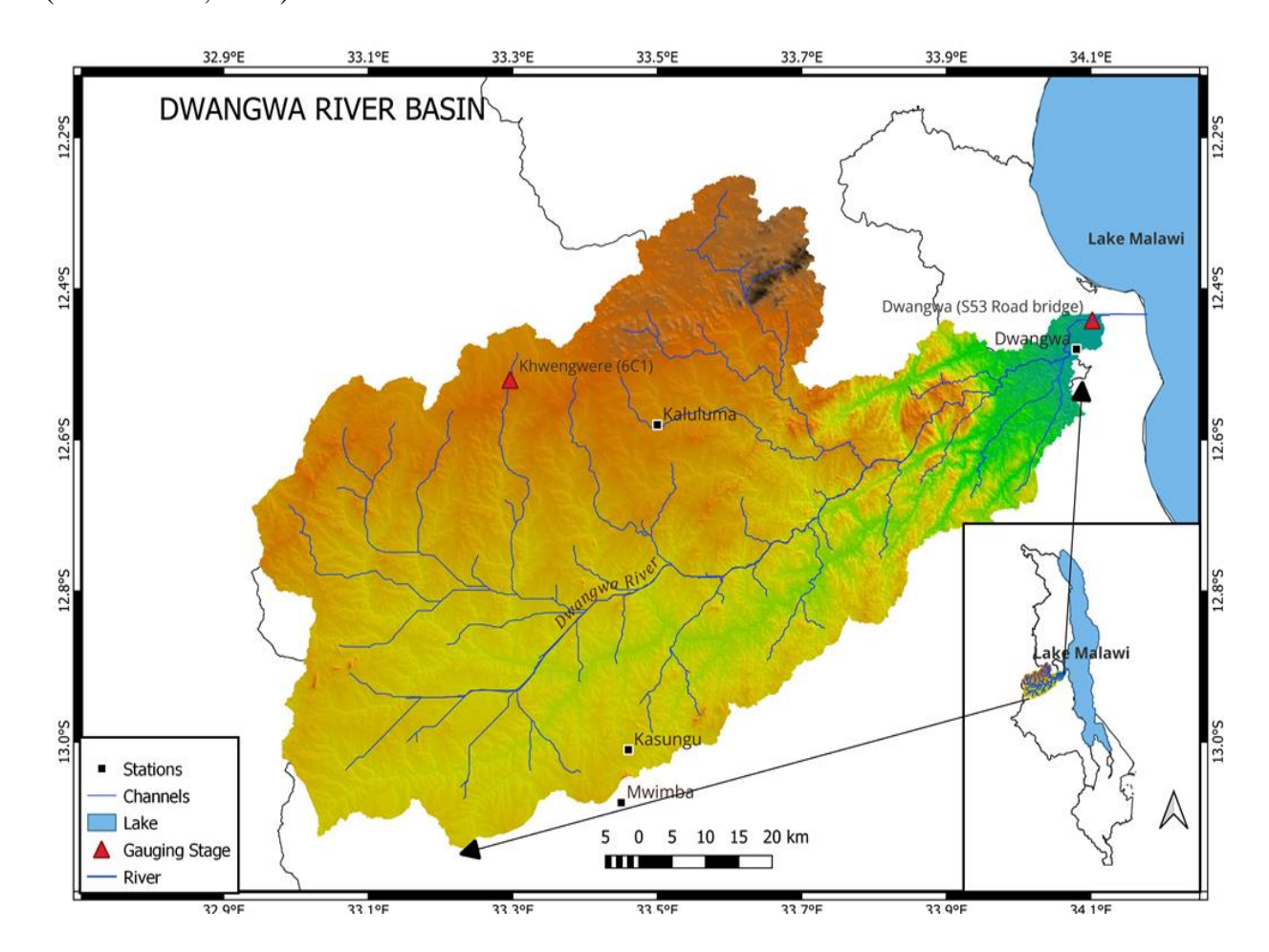


Figure 3 Dwangwa River Basin, showing rivers, stations and gauging stations.

## 3.3 Data Collection

## 3.3.1 Rainfall data

The Department of Climate Change and Meteorological Services of Malawi provided rainfall data from four separate gauging stations within the basin (Figure 3). Most of the stations in Malawi have missing data (Ngongondo et al. 2020). The data from the stations of Kaluluma, Mwimba, Kasungu, and Dwangwa, on the other hand, were complete. Data was collected during a 30-year period, from 1985 to 2015. The years were chosen because the World Meteorological Organization (WMO) recommended

30 years of data to look for evidence of climatic change in hydroclimatic time series (Ngongondo et al. 2010).

The quality of data for meteorological variables such as rainfall continues to be a challenge in data-scarce regions such as Malawi (Ngongondo et al. 2014). The DCCMS undertakes some data quality control checks before archiving their data (Ngongondo et al. 2014). In this study, we checked for randomness in the rainfall data series as part of the enhancement of data quality. The procedure ensures that data is independent and identically distributed, as required by some of the analysis procedures, such as trend tests.

Table 1 Active stations and co-ordinates in Dwangwa Basin

Station	Latitude (°S)	Longitude (°E)
Dwangwa	-12.48	34.08
Kaluluma	-12.58	33.50
Kasungu	-13.01	33.46
Mwimba	-13.08	33.45

## 3.3.2 River discharge data

Average monthly river discharge data for the upper and lower Dwangwa River Basin was collected from the Ministry of Irrigation and Water-Malawi, Department of Water Resources, from 1985 to 2009. The data is from two gauging stations at Kwengwere upper catchment and Dwangwa Road Bridge S53 lower catchment. Data was not available at Dwangwa Road Bridge S53 station from 1985 to 1986. The period from

2009 to 2015 had the longest period of missing data; hence, it was discarded for analysis. Many studies have recommended that for better spatial variability in streamflow analysis, data spanning more than 20 years can be desirable for trend analysis of streamflow (Gabremiceal et al. 2017).

It is argued that, despite the availability of numerous methods for filling in missing hydrological data, there is generally no single method that can be considered universally best (Mfwango et al. 2018). Further, it was mentioned that each method has its own advantages and disadvantages, depending on the characteristics of the data set. However, other factors, for instance, distance between stations, aerial coverage of each gauging stage, length of gap, the season, the climatic region, or the availability and data characteristics of the records, have significant influences on hydrological data estimates (Mfwango et al. 2018).

In this regard, the study used simple linear regression. In a case where missing data exists in the basin, missing flows can be estimated using nearby rivers that have data (Mfwango et al. 2018). The study used regression analysis to fill in the missing data. The method has been successfully utilised in hydrological studies (Mfwango et al. 2018). The discharge gauging stations had complete data from 1986 to 1989. There were big gaps between the series on both stations up until 2015. In other situations, data from one gauging station was used due to prolonged missing data at the stations. Therefore, for the hydrological response, the study used 24 years because of the long period of missing data in some years.

#### 3.3.3 El Niño Southern Oscillation data

ENSO data is based on sea surface temperature (SST), since it is the main indicator of El Niño and La Niña. SST data were obtained from the Niño 3.4 (SST 5N-5S, 170W-120W) regions of the tropical Pacific; this location is important to understand ENSO features (Salau et al. 2015). The Niño 3.4 data was downloaded from the website of the Climate Prediction Centre of the National Oceanic and Atmospheric Administration http://www.esrl.noaa.gov/psd/gridded/tables/monthly.htm (Salau et al. 2015).

According to the NOAA definition, an El Niño event occurs when the consecutive three-month running mean of the Niño 3.4 SST anomaly (SSTA) is above +0.5, while a La Niña event occurs when the SSTA is below -0.5. This index is extensively used because it captures several of the well-known El Niño and La Niña events. The JMA is a 5-month running mean of spatially averaged SST anomalies over the tropical Pacific (Arthur et al. 2002).

### 3.3.4 SST Anomalies

Nino 3.4 anomalies show that 1986, 1987, 1991, 1994, 1997, 2002, 2004, 2006, 2009, 2014, and 2015 had SST above +0.5, hence they were years that El Niño occurred (Figure 4). The SST anomaly of 1.6 recorded in 2014–2015 (+2.4) is the highest for the past 30 years. La Niña (-0.5) occurred in 1985, 1988, 1995, 1998, 1999, 2000, 2007, 2010, and 2011. While neutral years are 1989, 1990, 1992, 1993, 1996, 2001, 2012, and 2013 (Figure 4).

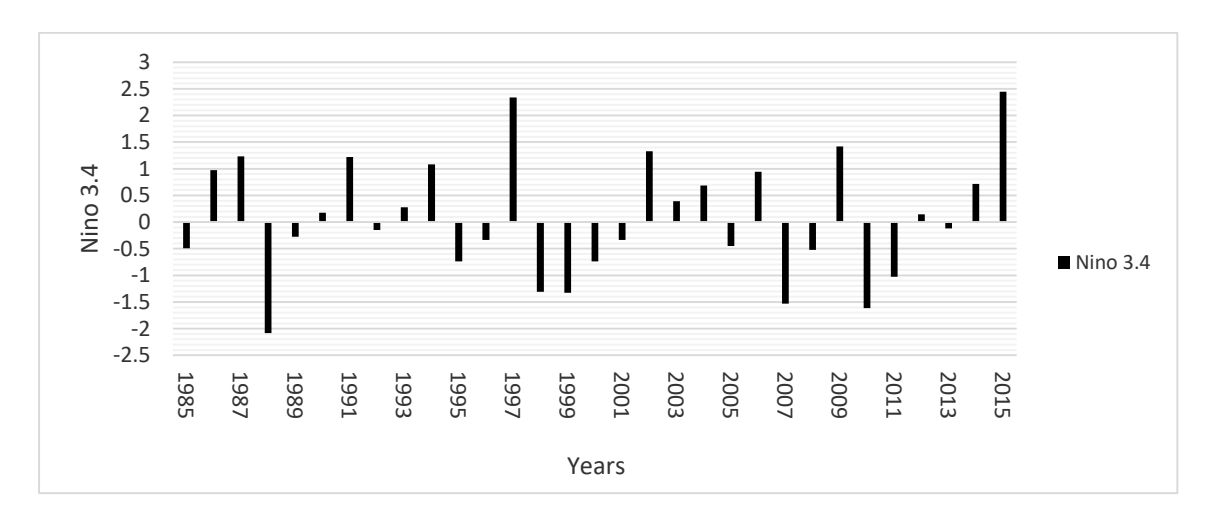


Figure 4 Nino 3.4 Anomaly showing years of El Niño, La Niña and Neutral Phase

# 3.3.5 Indian Ocean Dipole data

The study used the Dipole Mode Index (DMI) as an index to quantify the Indian Ocean Dipole (IOD). The DMI has been used in a number of studies (e.g., Behera et al., 2005; Muhati et al., 2007; Saji et al., 1999). When the DMI is positive, the phenomenon is

known as a positive IOD event, and when it is negative, it is a negative IOD event (Ogwang et al. 2015).

The Dipole Index available following Mode data is at the website: https://ds.data.jma.go.jp/tcc/tcc/products/elnino/index/iod\_index.html. Data was downloaded from the Tokyo Climate Centre, World Meteorological Organisation (WMO) Regional Climate Centre in RA II (ASIA), and a three-month average was calculated from October to December. The threshold was set at  $\pm 0.5$  standard deviation (Ji et al. 2021). The years with a standard deviation greater than  $\pm 0.5$  were classified as positive or negative. The study identified 1994, 1997, and 2015 as having positive IOD (Figure 5). While 1996, 1998, 2005, and 2010 are associated with negative IOD, Finally, 1986, 2000, 2002, 2004, 2008, and 2009 were neutral IODs (Figure 5).

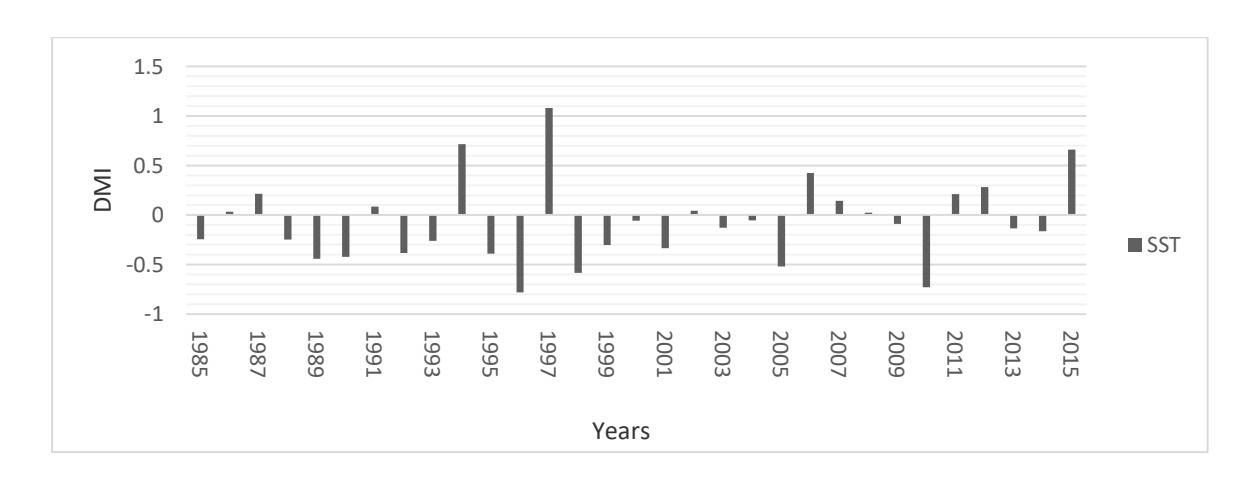


Figure 5 Indian Ocean Dipole Mode Anomaly

## 3.4 Data Analysis

The designated stations were validated by detecting outliers and homogeneity. The data was checked for randomness and persistence before applying the Mann-Kendall trend test. The temporal heterogeneity of monthly rainfall was checked using the Precipitation Concentration Index (PCI). PCI and coefficient variation were used to check for the variability of rainfall together.

## 3.4.1 Quality Control and Statistical Homogeneity Testing

The quality of data for meteorological variables such as rainfall continues to be a challenge in data-scarce regions such as Malawi. In the country, some stations have long-term missing data, while others have intermittently available data (Ngongondo et al. 2011). The data from the four stations provided had complete data. However, to ensure the quality of the data, it was tested for homogeneity. It is argued that sometimes climatic factors make the available data unrepresentative of the actual climate variation, and thus the conclusions of climatic and hydrological studies are sometimes biassed (Awiti et al. 2016). In this case, before the data was used, it was checked for (i) outliers, (ii) homogeneity, and (iii) randomness. These tests were made to check if the data is independent and identically distributed, as required by some of the analysis procedures.

### 3.4.2 Test for Outliers

In statistical approaches, all outlier detection methods are based on the principle that an outlier is an unsure observation that is slightly or fully out of the subject because the data is not generated by hypothetical models of the random variable (Mirzaei et al. 2014). The present study used the Grubbs test to detect outliers in rainfall and discharge data. Grubbs tests are statistical tests used to detect outliers that exist in a univariate data set using the mean, standard deviation, and tabulated criterion (Adikaram et al. 2015).

The Grubbs test is known as the maximum Normalised Residual Test or Extreme Studentised Deviation (ESD) Test, and it assumes that the data is normally distributed. It gives the result as a probability that indicates that the data belongs to the core population (Equation 1). If the investigated sample has some other, especially asymmetric distribution (e.g., lognormal), then these tests give false results (Grubbs, 1969). This test is based on the difference between the mean of the sample and the most extreme data, considering the standard deviation. (Adikaram et al. 2015). Equation (1) was used to calculate the outlier.

$$G = \frac{\max_{i=,\dots,N} |Y_i - \bar{Y}|}{S}$$
 Equation (1)

Where  $\bar{Y}$  is the sample mean of rainfall data,  $Y_i$  is the maximum of absolute differences between the values and s is the sample standard deviation. In this study, the G test statistic is compared to the critical value. The value below the critical value is kept, then the point is kept in the data set; it is not an outlier. When the value is greater than (>) then the point is considered an outlier.

The test was chosen because of its capability of identifying outliers at the 0.01 significance level. In addition, its robustness involves considering only the value of the data points but not the real order of the data (Adikaram et al. 2015).

Many studies have used the test to detect outliers (e.g., Sathish et al. 2017; Rahman et al. 2014). Stations identified with outliers were to be adjusted using the Tukey Fence Method (Tukey, 1977). First proposed by statistician John Turkey in 1970. This method is suggested to be good for data that is not normally distributed, like rainfall (Ngongondo et al. 2011). Then the Tukey fence range was created using ( $Q_1$ -1.5 IQR,  $Q_3$  + 1.5 IQR), where  $Q_1$  and  $Q_3$  are respectively the lower and upper quartile points.

## 3.4.3 Test for Homogenisation

There are many methods used for homogenisation of climatic station data, which include: double mass analysis, cumulative deviation method, worst-likelihood ratio test, maximum t-test, wilcoxon-Mann-Whiteney test, Craddock test, Potter's method, Kruskal-Wallis, and multiple analysis of series for homogenisation (MASH) (Costa and Soares, 2009). Despite the available statistical tests for homogenisation, it is argued that there is no single best technique to be recommended for homogeneity testing (Andang'o et al. 2011).

The contemporary study, therefore, opted to use the Standard Normal Homogenisation Test (SNHT) because it is argued to be more robust (Andang'o et al. 2011; Costas and Soares, 2009). Toreti et al. (2011) recommend that the SNHT be used with several references because of its limitations in discovering middle breaks in the data series. In this case, the study also used Buishand and Pettit's SNHT test for comparison purposes (Gyamfi et al. 2016).

The homogeneity test of climatic data is very crucial considering that non-climatic factors make available data misleading of the real climate variation, and thus the conclusions of climatic and hydrological studies may give unreliable results (Nsubuga et al. 2011). Data may be regarded as inhomogeneous if it has a gradual trend or a break in the mean or variance. Studies suggest that a change, however minor it may be, in the station environment or observation methods can artificially alter the mean measurements and make the series suspect or not homogeneous (Nsubuga et al. 2011; Gyamfi et al. 2016).

Toreti et al. (2011) recommend that the SNHT be used with several references because of its limitation in discovering middle breaks in the data series. In this case, the study also used Buishand and Pettit's SNHT test for comparison purposes (Gyamfi et al. 2016). The Buishand Range Test is capable of locating the period (month or year) where a break is likely. It is an advantage because it is more sensitive to breaks in the middle of a time series where the SNHT performs poorly (Wijngaard et al. 2003).

The Pettit Test, as a non-parametric test, is also capable of locating the period (month or year) where a break is likely. It is related to the Mann-Whitney statistic, and like other tests, it is more sensitive to breaks in the middle of a time series (Wijngaard et al. 2003). Essentially, a non-parametric test does not consider the normality of the series (Andang'o et al. 2011). The Pettitt Test is based on the rank (*r<sub>i</sub>*) of the *n* elements in the series (Pettitt, 1979).

The test considers that

$$U_k = 2\sum_{i=1}^k r_i - k(n+1), k = 1, ..., n$$
 Equation (2)

Beyond that, when a break takes place in the year *t*, the statistics of Pettit test is calculated using Equation (3).

$$U_t = \max_{1 \le k \le n} |U_k|$$
 Equation (3)

The SNHT is defined as (Alexanderson, 1986)

$$T_{max} = \max_{1 \le k \le n} \{ k\bar{z}_1^2 + (n-k)\bar{z}_2^2 \}, k = 1, \dots, n,$$
 Equation (4)

Where k is more probable to be the year for the break (matching to the maximum  $T_{max}$ ),  $\bar{z}_1$  is the mean of the series before the shift k, and  $\bar{z}_2$  the mean of the series from k+1 to n.

If  $Y_1, Y_2, ..., Y_n$  is the annual series, with  $\overline{Y}$  being the mean, the Buishand tests for homogeneity is based on the adjusted partial sums (Buishand, 1982) such that

$$S_k^* = 0, S_k^* = \sum_{i=1}^k (Y_i - \bar{Y}), k = 1, ..., n$$
 Equation (5)

When k=n,  $S_k^*=0$ , then  $S_k^*$  will float around zero if the series is homogenous, and there is no systematic pattern in the deviations of the series components from their mean.  $S_k^*$  also achieves an extreme (maximum or minimum) near the year k whenever a break is found on this k (Hansel et al. 2016).

For river discharge data series, however, raw data were visually inspected if it's complete. The stations were carefully checked for consistency in the upstream and downstream station data. This was achieved through the r squared (See Appendix C).

## 3.4.4 Test for randomness and persistence

There are varied methods used to determine the randomness and consistency of the data, for example: median crossing, turning points, rank difference, and autocorrelation (Aksoy, 2007). The monthly rainfall data, basin-wide mean monthly, and total annual rainfall were also checked for persistence before temporal analysis. A serial autocorrelation analysis was used to check for randomness and persistence. It has been used in many studies of temporal and spatial rainfall trend analysis (e.g., Ngongondo et al. 2011; Nsubuga et al. 2011).

Serial autocorrelation analysis correlates a time series dataset with itself at different time lags (Phillips et al. 2008). This is crucial for checking the randomness and periodicities of a time series dataset. Autocorrelation was performed on the monthly and total annual rainfall and river discharge data of individual stations in the catchment (Nsubuga et al. 2011). The study has used this method in order to make sure that the

rainfall and river discharge data series are free from influence from the earlier data series. Equation (6) was used for calculating the autocorrelation.

$$r_k = \frac{\sum_{i=1}^{N-k} (x_i - m)(x_{i+k} - m)}{\sum_{i=1}^{N} (x_i - m)^2}$$
 Equation (6)

Where  $r_k$  is the *lag-k* autocorrelation coefficient, m is the mean value of a time series  $x_i$ , is the number of observations, and is the time lag. If the calculated  $r_k$  is not significant at the 5% level, then the Mann-Kendall test is applied to the original values of the time series (Nsubuga et al. 2011). Where the calculated correlation is significant, the data sets were smoothed using a 3-year moving average to reveal more persistent trends (Wheeler and Martin-Vide, 1992; Nsubuga et al. 2011). The smoothed time series may be obtained as follows:

$$\overline{y}_t = \frac{y_t + y_{t-1} + \dots + y_{t-n-1}}{n}$$
 Equation (7)

Where y is the variable (such as rainfall or river discharge), t is the current time period (such as the current month) and n is the number of time periods in average.

## 3.4.5 Temporal trend analysis

Approaches used for detecting a trend in the time series can either be parametric or non-parametric. The Mann-Kendall (MK) test statistic was used for trend analysis (Mann, 1945; Kendall, 1975; full citations in Ngongondo et al. 2011). The test has been widely applied in various trend detection studies, including those of Kizza et al. (2009) and Nsubuga et al. (2011). The World Meteorological Organisation (WMO) recommends its use for trend analysis. Ngongondo et al. (2011) and Karmeshu (2012) argued that there are two benefits to using this test. It is a non-parametric test and does not require the data to be normally distributed. Second, the test has low sensitivity to abrupt breaks

due to its inhomogeneous time series. The test is insensitive to missing data and outliers. The test is recommended for non-normally distributed data series, such as rainfall. This study, therefore, applied the Mann-Kendall (MK) test to study temporal trends of the total annual and monthly (i.e., from November to April and May to October) rainfall and river discharge series as used by Ngongondo et al. (2011). The data for performing the Mann-Kendall analysis is supposed to be in a time-sequential order (Gemechu et al. 2015). The Mann-Kendall trend test is calculated according to Equation (8).

$$S = s = \sum_{k=1}^{n-1} \sum_{j=k+1}^{n} sgn(X_j - X_k)$$
 Equation (8)

With 
$$Sgn(X_j - X_k) = \begin{cases} +1, if(X_j - X_k) > 0\\ 0, if(X_j - X_k) = 0\\ -1, if(X_j - X_k) < 0 \end{cases}$$
 Equation (9)

Where  $X_j$  and  $X_k$  are sequential precipitation values in the month j, whereas; A positive value is an indicator of increasing (upward) trend and a negative value is an indicator decreasing (downward) trend. The slope of a linear trend is estimated with the non-parametric Sen's slope estimator's method (Gemeshu et al. 2015 references therein). It is the best method to detect trend because it is not affected by outliers and missing data (Gemeshu et al. 2015 references therein). The Sen's slope estimator was calculated using equation 9.

$$Q_i = \frac{x_j - x_k}{j - k}$$
 for  $i = 1 \dots N$  Equation (10)

Where  $x_j$  and  $x_k$  are data values at time j and k, j > k respectively. The median of these N values of  $Q_i$  is Sen's estimator slope. The presence of a statistically significant trend is evaluated using the Z value. To decide whether the null hypothesis is to be accepted or rejected, a test statistic is computed with a critical value obtained from a set of statistical tables. The null hypothesis is rejected if the absolute value of Z is

greater than  $Z_{1-a/2}$  and then the trend is considered as significant, Where  $Z_{1-a/2}$  is obtained from the standard normal distribution (Germeshu et al. 2015).

## 3.4.6 Rainfall and Areal Mean Characteristics

This study used annual and monthly mean rainfall data. Area average rainfall was calculated using the simple arithmetic average method. There are three classical methods of determining annual average rainfall: the arithmetic mean, the Thiessen polygon, and the isohyet (Limin et al. 2015). To determine the method to use for satisfactory analysis remains debatable (Limin et al. 2015). The study adopted the simple arithmetic method because it offers a simple technique for generating the area average rainfall (Limin et al. 2015).

The study used the precipitation concentration index (PCI) and coefficient variation (CV) as descriptors of rainfall variability in the Dwangwa River Basin (Hadgu et al. 2013). PCI was used to evaluate the varying weight of monthly rainfall relative to the total amount of rainfall (Li et al. 2010). This enabled an understanding of the monthly heterogeneity of rainfall amounts and their temporal trends. A modified version of PCI by Oliver (1980), cited in Nsubuga et al. (2011), and was applied:

$$PCI = 100 \times \frac{\sum_{i=1}^{12} P_i^2}{(\sum_{i=1}^{n} P_i)^2}$$
 Equation (11)

Where  $p_i$  is the rainfall amount of the ith month, calculated for each of the year (period) being considered.

PCI values below 10 indicate a uniform monthly rainfall distribution in the year, whereas values from 11 to 20 indicate seasonality in rainfall distribution. Values above 20 correspond to climates with substantial monthly variability in rainfall amounts

(Nsubuga et al. 2011). A higher precipitation concentration index value also indicates that precipitation is more concentrated during a few rainy months during the year and vice versa (Li et al. 2010; Nsubuga et al. 2011). The rainfall variability for representative meteorological stations was determined by calculating the coefficient of rainfall variation (CV) as the ratio of the standard deviation (SD) to the mean rainfall in a given period (CV %) when expressed as a percentage (Gemeshu et al. 2015). The coefficient of variation (CV) can be calculated using the following formula:

$$CV = \frac{\sigma}{x}$$
 Equation (12)

Where  $\sigma$  =Standard Deviation; x= mean based on the values of CV, (NMSA, 1996; Gemeshu et al. 2015), has classified the rainfall variability of an area as; CV<20% less variable, CV 20%-30% moderate variable and CV>30% high variable.

## 3.5 River discharge response to ENSO and IOD

The response of the river to global circulations of ENSO and IOD was checked by Simple Linear Regression.

$$y = B_0 + B_1 X + \epsilon$$
 Equation (13)

y is the predicted value of the dependent variable (y) for any given value of the independent variable (x).  $B_0$  is the intercept, the predicted value of y when the X is 0.  $B_1$  is the regression coefficient-how much we expect y to change as X increases (Equation 12). X is the independent variable (the variable we expect is influencing y). e is the error of estimate, or how much variation there is in our estimate of the regression coefficient. In this study, the discharge data at Dwangwa Bridge S53 and Kwengwere were regarded as dependent variables to Dipole Mode Index (DMI) and Nino 3.4 data for ENSO.

The idea was to check whether there was a positive or negative response to the ENSO and IOD episodes. The method is useful, as previous studies have adopted it in related studies (e.g., Pui et al. 2012). It mostly relies on the assumption of linearity in the relationships between variables. Since a comparison of correlations computed based on the Pearson product moment agrees well with the nonparametric rank-based correlation performed in this study, this suggests that the assumptions of linearity are justifiable.

## 3.6 Correlation analysis of rainfall and SST

Rainfall series from individual stations were correlated from 1985 to 2015. SST data from the Indian Ocean and Pacific from the Comprehensive Ocean Atmosphere Data Set (COADS) of the National Oceanic and Atmospheric Administration (NOAA) and the Tokyo Climate Centre World Meteorological Organisation (WMO) Regional Climate Centre in RA II (ASIA) were correlated with Malawi rainfall in the Dwangwa Basin. The main rainy season in Malawi is from November to April, and the dry season is from May to October (Ngongondo et al. 2010). The Pearson product moment correlation coefficient was applied to identify the relationship between rainfall, ENSO, and IOD (Chandimala and Zubair, 2007). The Pearson product moment correlation coefficient, r, between two-time series,  $x_{i \text{ and } y_i}$  is defined as in equation (14).

$$r = \frac{\sum_{i=1}^{N} (x_i - \bar{x})(y_i - \bar{y})}{\sqrt{\sum_{i=1}^{N} (x_i - \bar{x})^2 \sum_{i=1}^{N} (y_i - \bar{y})^2}}$$
 Equation (14)

Where  $\overline{x}$  and  $\overline{y}$  are the averages of time series  $x_i$  and  $y_i$ , respectively (Sitienai et al. 2017). The correlation coefficient r describes the degree of closeness to a linear relationship between two variables x and y (Sitienai et al. 2017). The value of r varies from -1 for a "perfect "out-of-phase correlation to +1 for a "perfect" in-phase correlation, and the coefficient of zero indicates that no linear relationship exists. To test whether the correlation is significant, the null hypothesis that the correlation is zero

and the alternative hypothesis that the correlation is nonzero were assumed (Sitienai et al. 2017). If the null hypothesis was valid, the relevant test variable (t) from equation (15) was the realisation of student (t) random variables with a mean of zero and n degrees of freedom (Sitienai et al. 2017). Based on this information, p-values were computed; p < 0.05 impelled the probability of discarding the null hypothesis and vice versa. The t-test statistics were used as given in equation (15).

$$t = \sqrt[r]{\frac{n-2}{1-r^2}}$$
 Equation (15)

#### **CHAPTER FOUR**

#### 4.0 RESULTS AND DISCUSSIONS

## 4.1. Rainfall variability

The maximum mean annual rainfall was observed in Dwangwa station at 1316 mm, with a mean monthly rainfall of 334 mm in March and a coefficient variation (CV) of 0.25. Kasungu station had the least mean annual rainfall of 778 mm, the highest average rainfall in January, and a CV of 0.21 (Table 2). Kaluluma station had a CV of 0.27 with a mean annual rainfall of 944 mm and the highest mean of 230 mm recorded in January. Mwimba station had a mean annual rainfall of 826 mm with a CV of 0.21 (Table 2). Dwangwa recorded the highest total annual rainfall of 2053 mm in 1988 and has been yielding a higher amount of rainfall every year than other stations for 30 years (Appendix B).

Dwangwa lies on the escarpment of Lake Malawi, which receives higher rainfall than lower-lying shadow areas. The mean annual rainfall of the Dwangwa Basin is 3150 mm with a standard deviation of 532 mm based on 30 years' cumulative data obtained from four stations (Appendix B). The analysis of the mean monthly rainfall of Dwangwa Basin indicates that rainfall during January is the highest (713 mm), which contributes to 22.6% of the annual rainfall of Dwangwa Basin (Appendix B). This is followed by February (706 mm), March (675 mm), and December (496 mm). The least amount of

rainfall is observed in June (7 mm), July (6 mm), August (3 mm), September (7 mm), and October (18 mm).

Table 2 of PCI, CV and annual mean of the rainfall stations

Station	Annual PCI (mean)	CV	Annual Mean in 30yrs (mm)
Dwangwa	23%	0.25	1316
Kasungu	30%	0.21	772
Kaluluma	22%	0.27	944
Mwimba	25%	0.21	826

# 4.2 Discharge characteristics

The highest discharge of 59 m3/s and 55 m3/s was found at S53 and Khwengwere, respectively (Figure 6). The highest mean monthly discharge in the two gauging stations was in February (Figure 6). River recession starts in the month of March, when the cold, dry season is approaching.

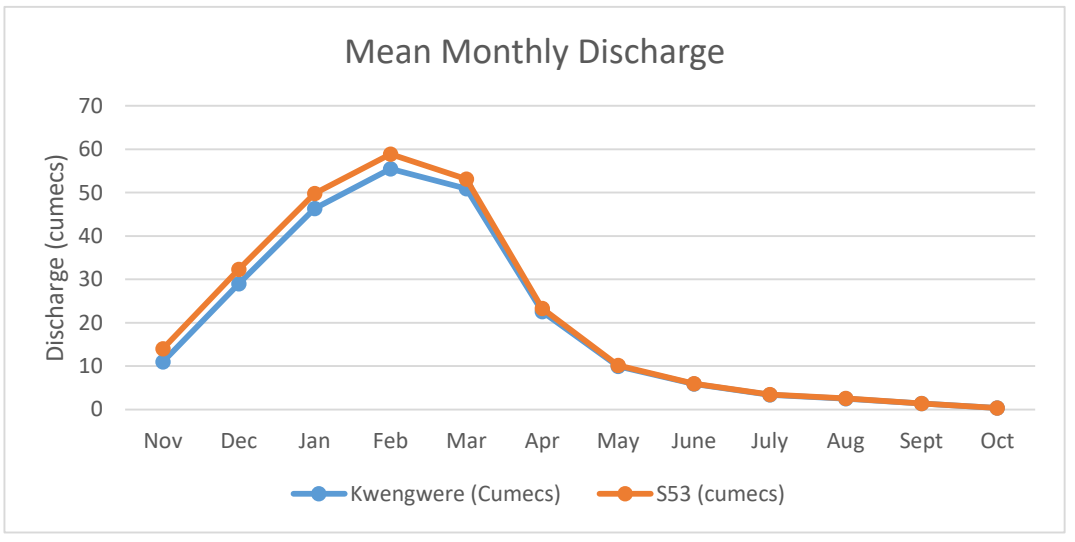


Figure 6 Mean monthly discharge of Dwangwa River Basin (1985-2009).

## 4.3 Rainfall data Validation

#### 4.3.1 Outlier detection

The results of the selected stations showed that the computed p-values of Kasungu, Dwangwa, and Mwimba were not statistically significant at the significance level of 0.05% and hence had no outliers (Table 3). Kaluluma was statistically significant at the 0.05% significance level, indicating suspected outliers. The outliers detected in the stations were adjusted using Tukey's face. Then neighbouring stations in the basin were used to compare the results. For instance, Kaluluma was used to compare with Kasungu and Mwimba. Yet Dwangwa was compared with Kaluluma. Similarly, river discharge data had suspected outliers at Dwangwa S53. This was adjusted using the Tukey face.

Table 3 Grubbs test for Outliers/Two tailed test.

Station	P-value (Two tailed)	99% confidence interval	Alpha
		on the p-value	
Kasungu	0.702	0.701,0.703	0.05
Mwimba	0.609	0.608,0.610	0.05
Dwangwa	0.711	0.710,0.713	0.05
Kaluluma	0.052	0.051,0.052	0.05

## **4.3.2** Homogenisation test

The annual data series from individual stations were further tested for homogeneity using Pettitt's Test, the Standard Normal Homogeneity Test, and Buishand's Test

(Table 4). The null hypothesis H0 of the data being homogeneous was tested against an alternative hypothesis Ha, where there is a date at which there was a change in the data. The P-values were computed using a 99% confidence interval. The results indicated that all the stations were not statistically significant at 0.05% significance levels (Table 4). Therefore, stations are considered homogeneous. River discharges displayed that the data was not homogeneous at the annual scale as it had jumps. However, the study checked monthly mean homogeneity, and the data had a suspect in the month of November only. The data in the month of November was treated using a three-month moving average. In that case, the data was regarded as homogeneous and useful.

Table 4 Homogeneity tests using Pettitt's, Buishand and SNHT

Stations	Pettitt's test (p-value)	Buishand test (p-value)	SNHT (p-value)
Kasungu	0.378	0.224	0.337
Mwimba	0.726	0.743	0.561
Kaluluma	0.360	0.208	0.350
Dwangwa	0.746	0.221	0.347

## 4.3.3 Autocorrelation Analysis of Annual and Monthly Series

Autocorrelation function results indicated that except at 0 lag which is always 1 almost all autocorrelations up to lag-12 are not significant. Serial correlation both monthly and annually of the rainfall and river discharge data were considered to be random and independent.

# 4.4 Temporal Trend Analysis

## 4.4.1 Annual and monthly rainfall series trend

The Mann-Kendall test was employed to detect trends in the data series. Except Kaluluma (Table 6) all the stations Mwimba (Table 1), Kasungu (Table 7), and Dwangwa (Table 8) displayed a statistically insignificant decreasing (0.05) trend monthly. At Mwimba, the months of March and October had statistically significant negative and positive trends, respectively (Table 5). While Kasungu displayed a non-significant increase in rainfall in August and February (Table 7). Yet at Kaluluma the month of December and February had insignificant decrease in rainfall (Table 6) the rest displayed insignificant increase in rainfall.

Table 5 Summary of Monthly Mann Kendall test for Mwimba station

Series\Test	Kendall's tau	p-value	Sen's slope
JUL	-0.121	0.414	0.000
AUG	0.201	0.173	0.000
SEP	0.256	0.081	0.000
OCT	0.298	0.041	0.000
NOV	-0.002	0.986	0.000
DEC	0.218	0.083	1.814
JAN	0.006	0.961	0.031
FEB	-0.065	0.618	-0.999
MAR	-0.310	0.012	-3.298
APR	-0.198	0.117	-1.797
MAY	-0.223	0.076	-0.407
JUN	-0.153	0.276	0.000

Table 6 Summary of Mann Kendall test for Kaluluma station

<b>Series\Test</b>	Kendall's tau	p-value	Sen's slope
JUL	0.270	0.044	0.000
AUG	0.243	0.068	0.000
SEP	0.308	0.022	0.000
OCT	0.116	0.377	0.000
NOV	0.165	0.191	0.954
DEC	-0.165	0.191	-2.050
JAN	0.137	0.280	1.483
FEB	-0.004	0.987	-0.041
MAR	0.060	0.641	0.725
APR	0.180	0.149	1.574
MAY	0.195	0.133	0.253
JUN	0.260	0.047	0.134

Table 7 Summary of Mann Kendall test for Kasungu

<b>Series\Test</b>	Kendall's tau	p-value	Sen's slope
JUL	-0.145	0.310	0.000
AUG	-0.028	0.847	0.000
SEP	0.011	0.938	0.000
OCT	-0.082	0.537	0.000
NOV	-0.236	0.058	-1.367
DEC	-0.069	0.596	-0.685
JAN	-0.032	0.810	-0.391
FEB	-0.153	0.226	-1.831
MAR	-0.060	0.641	-0.473
APR	-0.002	0.987	-0.003
MAY	-0.139	0.324	0.000
JUN	-0.008	0.957	0.000

Table 8 Summary of Mann Kendall test for Dwangwa station

<b>Series\Test</b>	Kendall's	p-value	Sen's slope
	tau		
JUL	-0.097	0.475	0.000
AUG	0.003	0.985	0.000
SEP	-0.053	0.706	0.000
OCT	-0.030	0.817	0.000
NOV	-0.114	0.363	-0.618
DEC	-0.153	0.226	-2.183
JAN	-0.008	0.962	-0.163
FEB	0.125	0.326	2.264
MAR	-0.077	0.552	-1.738
APR	-0.161	0.202	-2.448
MAY	-0.539	< 0.0001	-0.408
JUN	-0.152	0.262	0.000

## 4.4.2 Areal mean monthly and annual total trend

In the Dwangwa basin, an insignificant decrease in rainfall was found from February to May (Table 9). Again, the months of November and December were dominated by an insignificant decrease in rainfall. Moreover, the months that are associated with low rainfall during the dry season are dominated by an insignificant increase in rainfall (Table 9). Generally, all the months that are associated with an increased amount of rainfall, except January, are dominated by an insignificant decrease in rainfall in the basin (Table 9). An insignificant decrease in rainfall is found annually in the Dwangwa Basin. Based on this understanding, it can be said that rainfall is decreasing annually in the basin. Again, there is a decrease in rainfall during the rainy season

Table 9 Summary of Mann Kendall trend tests for areal mean monthly and annual total trend

	Kendall's		
Series\Test	tau	p-value	Sen's slope
JAN	0.020	0.884	0.638
FEB	-0.036	0.783	-1.074
MAR	-0.181	0.149	-5.918
APR	-0.190	0.132	-4.665
MAY	-0.347	0.006	-1.697
JUN	0.069	0.601	0.006
JUL	0.078	0.547	0.031
AUG	0.224	0.080	0.051
SEP	0.150	0.248	0.025
OCT	0.067	0.603	0.120
NOV	-0.234	0.062	-3.006
DEC	-0.065	0.615	-2.231
ANNUAL			
TOTALS	-0.238	0.058	-24.636

# 4.5 Mean Annual River Discharge

Mean annual river discharge at Kwengwere displayed an insignificant increase in discharge (Figure 7). Similarly, the gauging station at S53 displayed an increase in trend pattern in the Dwangwa River Basin (Figure 8).

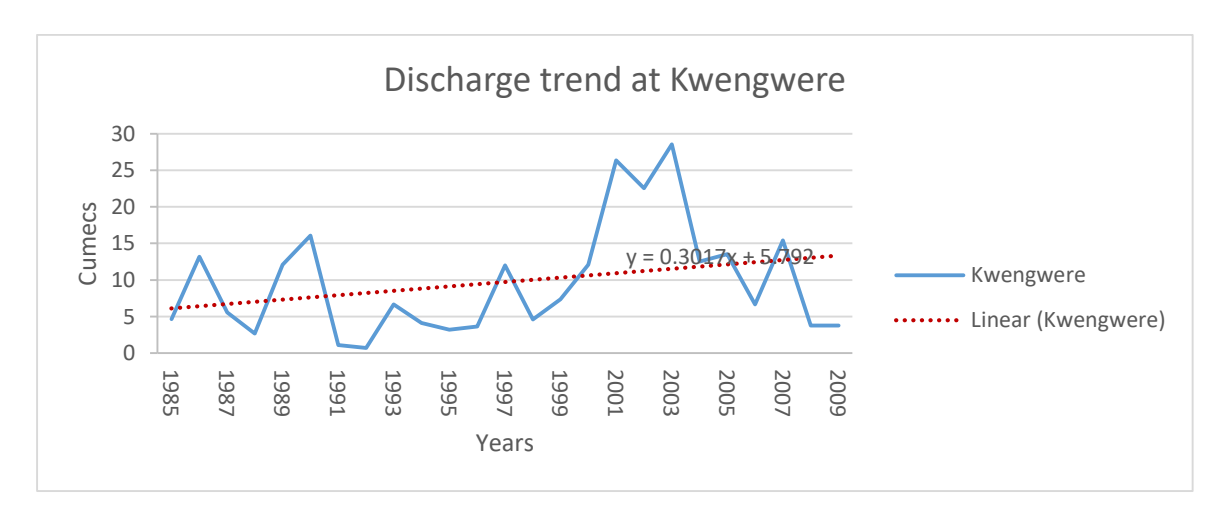


Figure 7 Mean Annual Discharge at Kwengwere

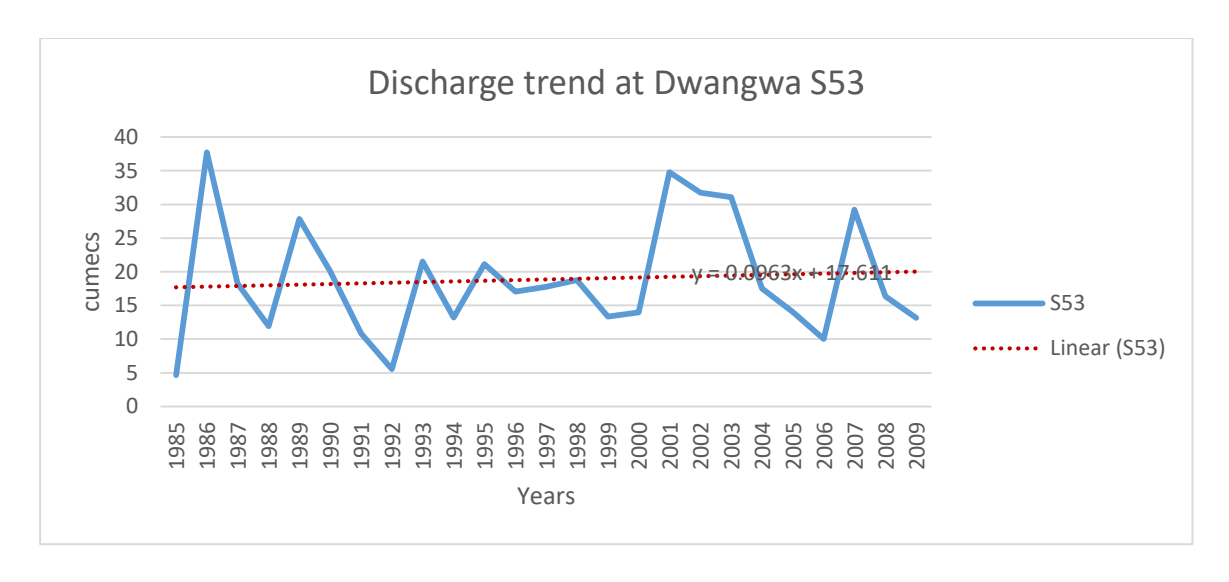


Figure 8 Mean Annual Discharge at S53.

# 4.6 Correlation between SST and Rainfall in Dwangwa River Basin

The study applied correlations over the Hot Wet Season (October, November, December, and January) and SST during El Niño, La Niña and Neutral years. The Analysis involved selecting the years based on the SST anomalies.

#### 4.6.1 ENSO with rainfall and areal mean

The correlations were conducted on an annual scale from October, November, December, and January (ONDJ). The results exhibited a negative, insignificant correlation between rainfall and Nino 3.4 during Strong El Niño (Table 9). However, the stations of Kasungu and Mwimba had an insignificant positive correlation with Nino 3.4. The study suggests that rainfall is higher during El Niño in Kasungu and Mwimba Stations, unlike during the La Niña Phase. However, the whole basin exhibited a strong negative and insignificant correlation between rainfall and Nino 3.4 during El Niño (Table 10). Whereas, La Niña phase is associated with a strong positive insignificant correlation with rainfall in DRB. (Table 11). Moreover, during the neutral phase, positive insignificant correlations dominated in the basin (Table 12). Though the station of Mwimba demonstrated an insignificant correlation.

Table 10 Correlation between Rainfall and Nino 3.4 during El Niño Years

Variables	Kasungu	Dwangwa	Mwimba	Kaluluma	Areal	Nino 3.4
Kasungu	1	0.045	-0.862	-0.427	0.031	0.277
Dwangwa	0.045	1	-0.545	0.884	1.000	-0.948
Mwimba	-0.862	-0.545	1	-0.090	-0.533	0.248
Kaluluma	-0.427	0.884	-0.090	1	0.891	-0.987
Areal	0.031	1.000	-0.533	0.891	1	-0.952
Nino 3.4	0.277	-0.948	0.248	-0.987	-0.952	1

*Values in bold are different from 0 with a significance level alpha=0.05* 

Table 11 Correlation between Rainfall and Nino 3.4 during La Niña Years

Variables	Kasungu	Dwangwa	Mwimba	Kaluluma	Areal	Nino 3.4
Kasungu	1	0.761	0.697	0.738	0.748	0.876
Dwangwa	0.761	1	0.996	0.999	1.000	0.353
Mwimba	0.697	0.996	1	0.998	0.997	0.264
Kaluluma	0.738	0.999	0.998	1	1.000	0.321
Areal	0.748	1.000	0.997	1.000	1	0.334
Nino 3.4	0.876	0.353	0.264	0.321	0.334	1

Values in bold are different from 0 with a significance level alpha=0.05

Table 12 Correlation between Rainfall and Nino 3.4 during Neutral phase

Variables	Kasungu	Dwangwa	Mwimba	Kaluluma	Areal	Nino 3.4
Kasungu	1	0.901	-0.892	0.395	0.909	0.661
Dwangwa	0.901	1	-1.000	0.755	1.000	0.921
Mwimba	-0.892	-1.000	1	-0.769	-0.999	-0.929
Kaluluma	0.395	0.755	-0.769	1	0.742	0.951
Areal	0.909	1.000	-0.999	0.742	1	0.913
Nino 3.4	0.661	0.921	-0.929	0.951	0.913	1

*Values in bold are different from 0 with a significance level alpha=0.05* 

## 4.7 Correlation between Dipole Mode Index (DMI) and rainfall

Rainfall exhibited a strong, insignificant negative correlation between rainfall and DMI during positive IOD (Table 13). However, the station of Kasungu displayed a positive but insignificant correlation with IOD. Although area rainfall displayed a negative, insignificant correlation between DMI and rainfall during the positive IOD (Table 13), during the negative IOD, a positive but insignificant correlation was revealed between rainfall in the Dwangwa River Basin and the negative IOD (Table 14). Yet during the neutral phase, rainfall displayed a very strong positive correlation with IOD, though it was insignificant. It was the station of Kaluluma that had a significant positive correlation with IOD (Table 15).

Table 13 Correlation between Rainfall and DMI during Positive IOD

Variables	IOD (+)	Kasungu	Dwangwa	Mwimba	Kaluluma	Areal
IOD (+)	1	0.880	-0.956	-0.526	-0.652	-0.702
Kasungu	0.880	1	-0.981	-0.866	-0.934	-0.956
Dwangwa	-0.956	-0.981	1	0.753	0.846	0.881
Mwimba	-0.526	-0.866	0.753	1	0.988	0.975
Kaluluma	-0.652	-0.934	0.846	0.988	1	0.998
Areal	-0.702	-0.956	0.881	0.975	0.998	1

Values in bold are different from 0 with a significance level alpha=0.05

Table 14 Correlation between Rainfall and DMI during Negative IOD

Variables	IOD (-)	Kasungu	Dwangwa	Mwimba	Kaluluma	Areal
IOD (-)	1	0.947	0.525	0.115	0.748	0.883
Kasungu	0.947	1	0.226	0.308	0.613	0.689
Dwangwa	0.525	0.226	1	-0.548	0.707	0.862
Mwimba	0.115	0.308	-0.548	1	-0.559	-0.255
Kaluluma	0.748	0.613	0.707	-0.559	1	0.851
Areal	0.883	0.689	0.862	-0.255	0.851	1

Values in bold are different from 0 with a significance level alpha=0.05

Table 15 Correlation between Rainfall and DMI during Neutral Phase

Variables	IOD (o)	Kasungu	Dwangwa	Mwimba	Kaluluma	Areal
IOD (o)	1	0.235	0.747	-0.689	0.908	0.756
Kasungu	0.235	1	0.803	-0.512	0.020	0.809
Dwangwa	0.747	0.803	1	-0.655	0.491	0.991
Mwimba	-0.689	-0.512	-0.655	1	-0.750	-0.714
Kaluluma	0.908	0.020	0.491	-0.750	1	0.544
Areal	0.756	0.809	0.991	-0.714	0.544	1

Values in bold are different from 0 with a significance level alpha=0.05

# 4.8 River discharge response to ENSO and IOD

Using simple linear regression, both Kwengwere and Dwangwa Bridge S53 displayed a decrease in discharge during the El Niño phase (Figure 9). Whereas during the La Niña phase, river discharge displayed an increased pattern (Figure 10). However, the neutral phase displayed a decrease in river discharge in the

basin (Figure 11). The study revealed mixed responses between discharge and IOD in the Dwangwa River Basin. A negative trend was witnessed in discharge during positive IOD (Figure 12). During negative IOD, the Dwangwa River Basin witnessed an increase in annual river discharge (Figure 13). However, during the neutral phase, the catchment had mixed results in the upper and lower catchments (Figure 14). The upper catchment at Kwengwere is associated with an increase in river discharge during the neutral phase. Yet discharge at Dwangwa Road Bridge S53 displayed a slight decrease in river discharge (Figure 11).

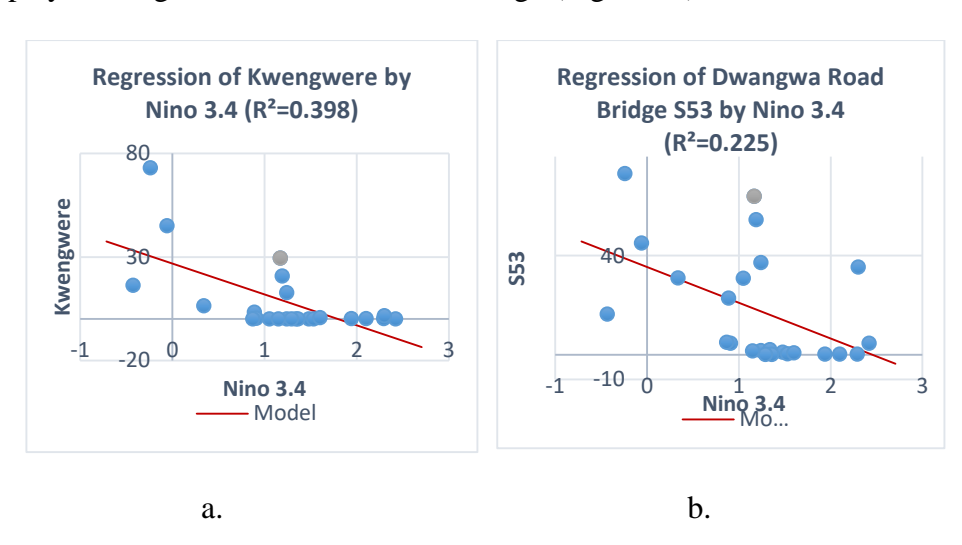
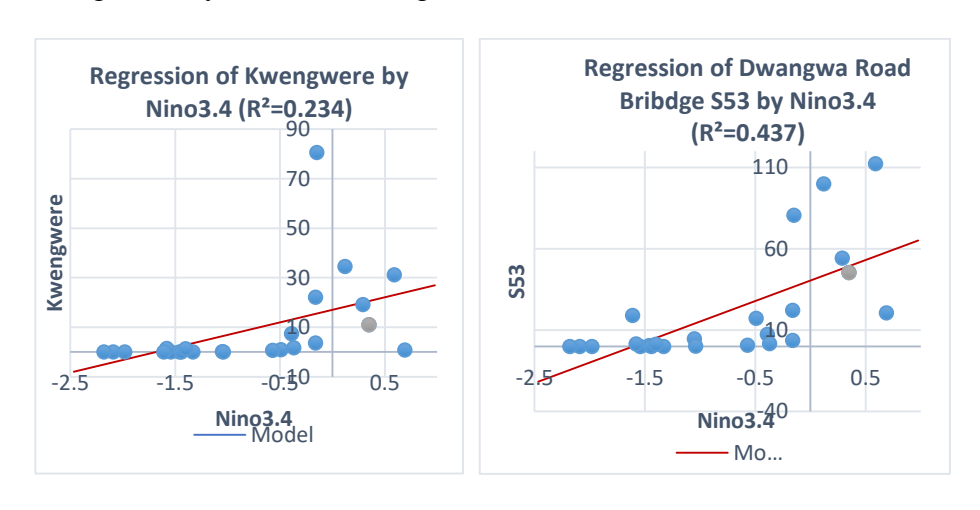


Figure 9 a. and b. are Regression of Kwengwere and Dwangwa Road Bridge S53 by Nino 3.4 during El Niño



b

Figure 10 a. and b. are Regression of Kwengwere and Dwangwa Road Bridge S53 by Nino 3.4 during La Niña

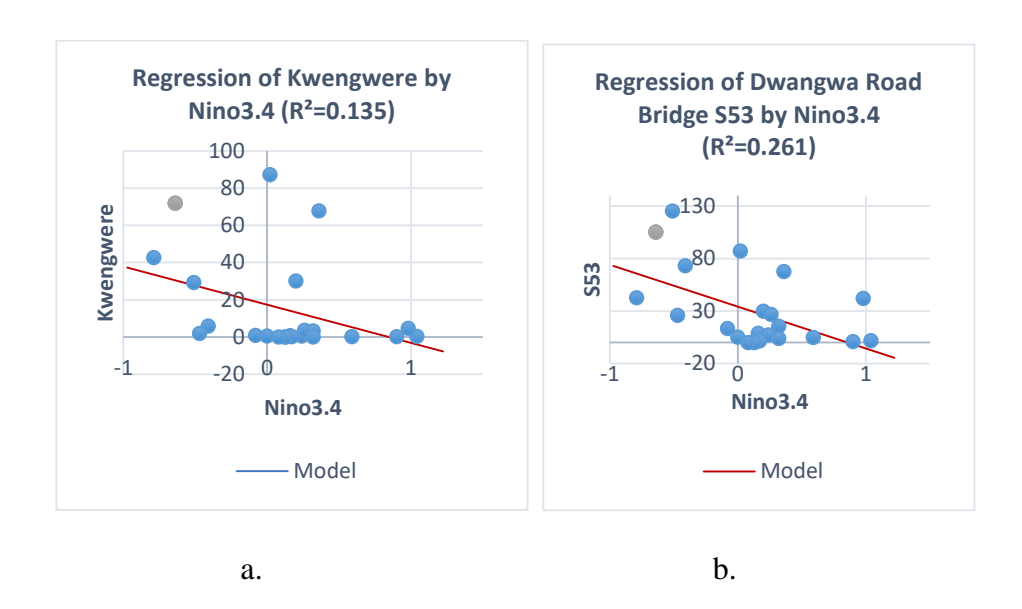


Figure 11 a. and b. are Regression of Kwengwere and Dwangwa Road Bridge S53 by Nino 3.4 during Neutral Phase

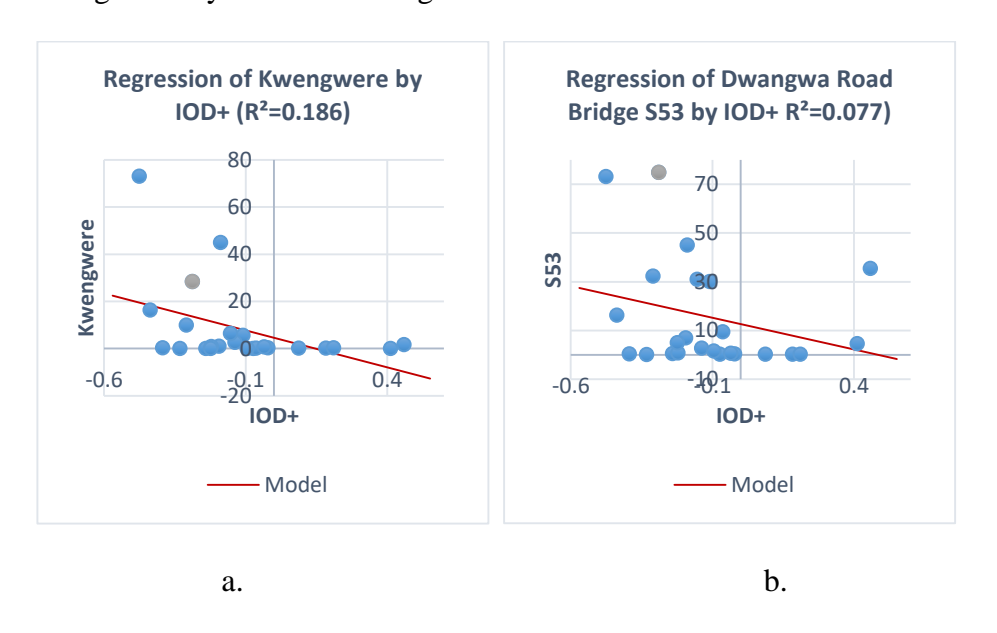


Figure 12 a. and b. are Regression of Kwengwere and Dwangwa Road
Bridge S53 by IOD+

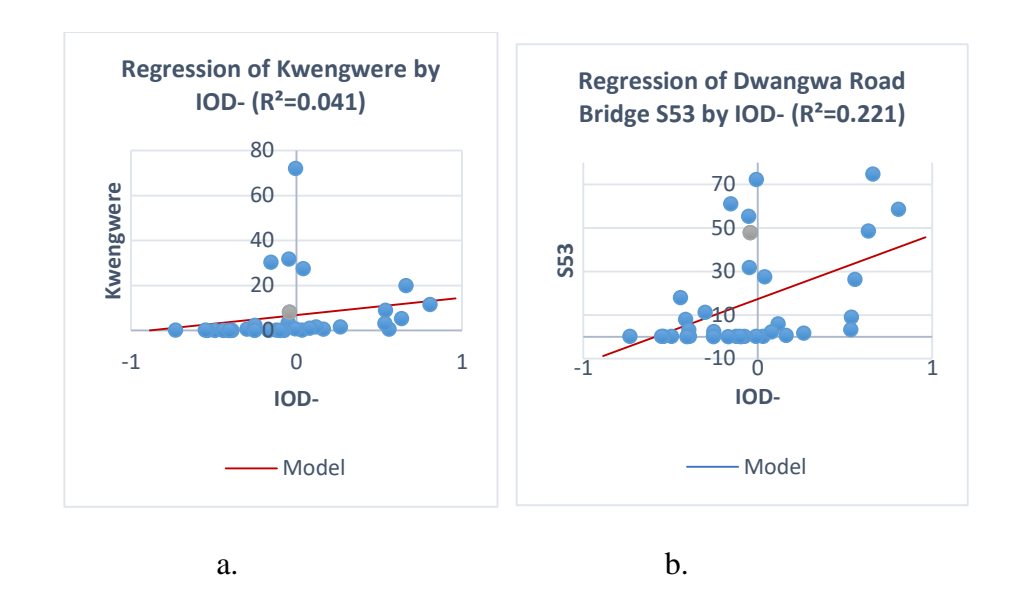


Figure 13 a. and b. are Regression of Kwengwere and Dwangwa Road Bridge S53 by Negative IOD

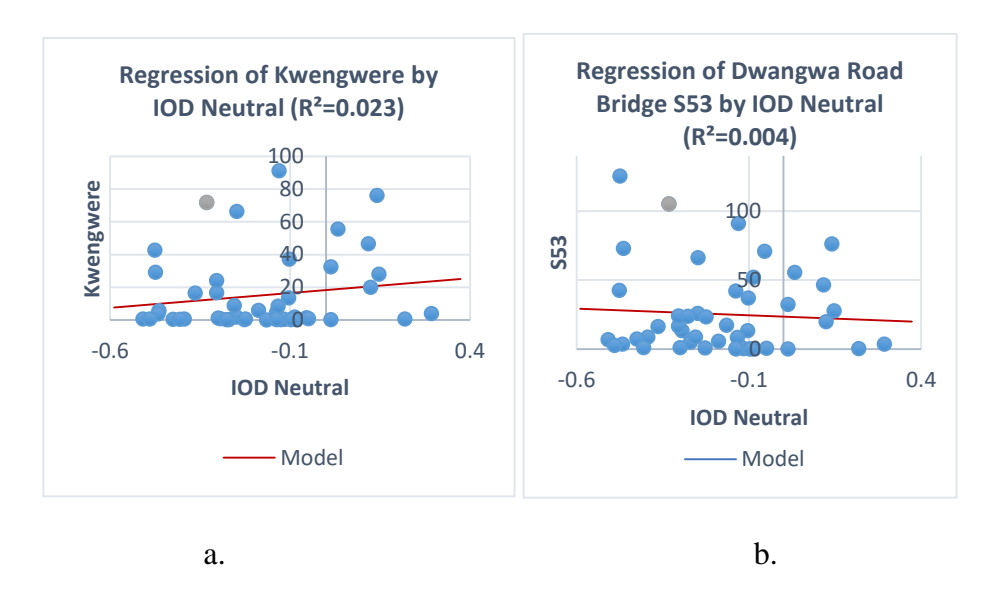


Figure 14 a. and b. are Regression of Kwengwere and Dwangwa Road Bridge S53 by Nino 3.4 during Neutral Phase

#### 4.9 Discussion of results

The study included a variety of findings that were synthesised for discussion in the study. The first section discusses climate variability in the DRB and trend patterns, while the last portion examines the link between SST and hydro-climatic parameters in the basin. Thus, the study sought to demonstrate that the catchment does not experience climate variability and that global circulations have no effect on climate variability and river discharge in the Dwangwa River Basin. The study examined the variability of rainfall from 1985 to 2015, representing a period of 30 years.

### 4.9.1 Climate variability in Dwangwa River Basin

The Dwangwa basin watershed has an average CV of 0.24, suggesting that rainfall doesn't vary considerably from year to year. The smaller CV in the Dwangwa River Basin shows that rainfall is still higher in the area. According to Ngongondo et al. (2011), areas with heavy rainfall had reduced inter-annual variability in all months of Malawi. As a result, based on the lowest CV, our analysis demonstrated that the watershed is still not very variable. Furthermore, Nsubuga et al. (2011) found that locations with a CV greater than 30% are more prone to experience frequent and severe droughts and floods. However, drought patterns were not visible in the Dwangwa River Basin during the years 1985 and 2015.

Further, the stations in the basin had a Precipitation Concentration Index (mean) between 20% and 30%, indicating rainfall distribution to be highly variable temporally within the years. PCI values below 10 indicate a uniform monthly rainfall distribution in the year, whereas values from 11 to 20 indicate seasonality in rainfall distribution. Values above 20 correspond to climates with substantial monthly variability in rainfall

amounts (Nsubuga et al. 2011). A higher precipitation concentration index value also indicates that precipitation is more concentrated during a few rainy months during the year and vice versa (Li et al. 2010; Nsubuga et al. 2011). The variability within the year could be emanating from seasonality of rainfall in the region.

According to the findings of Ngongondo et al. (2011) in the study that evaluated the spatial and temporal characteristics of rainfall in Malawi, the PCIs were found to be equal to the rainfall patterns of the Dwangwa River Basin. Moreover, the stations with the highest mean annual rainfall, especially those with relatively lower concentration indices, were associated with higher inter-annual rainfall variability.

Along with the same findings, the Dwangwa River Basin was associated with low concentration indices. This study is also in tandem with the findings of Ngongondo et al. (2011) based on the distribution of PCI in the country; low PCI indices were found around the central region of Malawi, where this Drainage Basin straddles. The analysis displays that there is temporal rainfall variability in the basin. Similarly, it was demonstrated by Tadeyo et al. (2020) that central Malawi has more variability interms of rainfall than Southern Malawi.

The study also looked at trends in river discharge. The investigation revealed that the river's yearly flows are decreasing. Ngongondo et al. (2014) observed similar findings, observing a decline in runoff throughout the nation from 1971 to 2000. Furthermore, Mbano et al. (2009) discovered a decrease in river flow in the Mulunguzi and Namadzi catchment basins. In general, the study found that the whole drainage basin is seeing a decline in rainfall and flow, both yearly and monthly. The decrease in river flow could

be associated with an increase in human activities, which has resulted in some tributaries not being sustainable throughout the year.

## 4.9.2 Climate trend in Dwangwa River Basin

At a 0.05% significance level, the analysis found that all of the stations are dominated by insignificant negative trends both monthly and annually. This shows that rainfall patterns are declining in the drainage basin. This finding is similar to earlier studies, though they looked at rainfall across Malawi (Ngongondo et al. 2011; Kumbuyo et al. 2010).

Comparable to what Ngongondo et al. (2011) and Kumbuyo et al. (2010) studied in the variability of rainfall time series in Malawi the studies reported that stations along the rift valley escarpment get more rainfall, resulting in a tropical environment that favours rainfall. Dwangwa station has recorded the most rainfall over a thirty-year period. This can be linked to local meteorological conditions in the basin, which show that the stations along the lakeshore and southeast of the nation had the most rainfall recorded. However, the rift valley causes the elevation of water vapour from Malawi's lake, resulting in relief rains in the area. This might be the reason for an increase in rainfall at Dwangwa station.

# 4.9.3 Impact of ENSO and IOD on Rainfall in Dwangwa River Basin

The study found that there is a negative, insignificant correlation between warmer SST at Nino 3.4 (El Niño) and rainfall (ONDJ) in the basin. During La Niña, rainfall displayed an increased pattern in most stations in the Dwangwa River Basin. The findings are similar to the study by Thulu et al. (2017), which displayed that El Niño seasons had a decreasing rainfall average trend over Malawi. The study further noted

the progression of El Niño rainfall seasons to longer dry spells in the country. However, the study also acknowledged that during this El Niño season, other areas receive abovenormal average rainfall.

The present study also noted similar patterns in the stations of Kasungu and Mwimba, which presented positive correlations during El Niño. Further, La Niña presented a stronger relationship with rainfall compared to El Niño. This displays that rainfall is more influenced by La Niña than La Niña. The Dwangwa River Basin showed that there is a negative rainfall relationship with El Niño. Yet during La Niña, rainfall has had a strong correlation with sea surface temperature in the Pacific.

The findings suggest that the Dwangwa River Basin lies in the transition zone. According to available literature in Malawi, northern Malawi lies near the transition zone of ENSO influence, with opposing centres of action in southern and eastern Africa (Jury and Mwafulirwa, 2002). This is to say that northern Malawi experiences different rainfall conditions during El Niño events from southern Malawi (Jury and Mwafulirwa, 2002; Thulu et al. 2020). These findings confirm that larger global driving forces have a role to play in driving rainfall mechanisms in the country. Neukom et al. (2014) indicated that the precipitation record for the last 200 years from southern Africa (south of 10° S) confirms a strong relationship between the summer rainfall and SSTs.

Saji and Yamagata (2003) have used partial correction analysis to show that positive Indian Ocean Dipole (IOD) events rather than El Niño dominate the enhancement of east African rainfall. The study found the opposite of that, as negative IOD had a strong positive correlation, though insignificant in the catchment, in the rainfall of October to

December from 1985 to 2015. Yet the warm IOD phase in the catchment at most stations shows that it contributes to low rainfall in the catchment.

The study used linear regression to check the response of river discharge during different SST conditions, both in the Pacific and Indian Oceans. It was found that the results agree with what was found in the correlation of rainfall with ENSO and IOD. During El Niño, the Dwangwa River Basin experiences a decrease in river discharge, though it is insignificant (see Figure 9). And the opposite was found during the cold phase of SST at Nino 3.4. A mixed response is noted during the neutral years. Furthermore, the river discharge response to global circulations augments the findings of the correlations. A negative, non-significant response was found during El Niño years, which confirms that El Niño results in decreased rainfall and river discharge in the catchment.

This could be due to droughts, which result in the drying of small rivers, resulting in low flow. Thulu et al. (2020) found a decrease in the Shire River flow rate during the El Niño phase. However, the findings are contrary to the studies conducted by Alemaw and Chaoka (2005). The studies of Alemaw and Chaoka (2005) investigated 502 rivers gauged from 1950 to 1998 in nine countries of the Southern African region. They found a strong and nearly strong positive linear correlation between annual discharges and warm seasonal ENSO indices, explained by the sea level pressure (SLP) data.

On the other hand, during La Niña, there is a positive but insignificant response in river discharge. Moreover, IOD had an overwhelming impact on the rainfall regime in the basin, especially during negative IOD. Low SST in the Indian Ocean contributes to

increased rainfall and discharge in the basin. Yet a positive IOD results in a decreased response in river discharge, though not significant. Contrary to this, the studies by Ngongondo et al. (2020) found that IOD had a non-significant impact on the variation of the Lake Malawi level. Additionally, Ogwang et al. (2021) agree that the rainfall pattern in Southern Africa is influenced by the Indian Ocean Dipole.

Generally, the results show that rainfall does not vary greatly in the catchment and that there is an insignificant decrease in rainfall in the catchment. El Niño contributes to decreased rainfall and river discharge in the catchment, yet La Niña means high rainfall and low river discharge. Negative IOD correlates positively with the rainfall regime in the basin and contributes to an increased discharge response. Positive IOD, however, contributes to low rainfall and river discharge responses in the basin.

#### **CHAPTER FIVE**

#### 5.0 CONCLUSION AND RECOMMENDATIONS

Global circulations driven by tropical ocean SSTs are among the factors influencing climate patterns in various parts of the world. Therefore, it is imperative to study the implications it exerts on local catchments in order to enhance adaptive mechanisms to climate change, environmental planning, and water resource management. As a result, the current study sought to investigate the effects of ENSO and IOD on hydroclimatic variability in the Dwangwa River Basin. It specifically studied climate variability in the Dwangwa River Basin, assessed the influence of ENSO and IOD on climate variability, and investigated the river discharge response in connection to ENSO and IOD.

The study found CV below 30%, typical of climates with moderate monthly rainfall variability. While PCI ranged between 20% and 30%. Suggesting a highly variable temporal intra-annual rainfall distribution in DRB. Moreover, the Mann-Kendal test statistics showed insignificant annual rainfall trends. Further, rainfall and discharge exhibited a decreasing trend, though insignificant, in all the stations of Kaluluma, Kasungu, Dwangwa, and Mwimba. The total annual average rainfall displayed that rainfall is declining insignificantly in the Dwangwa River Basin. Generally, speaking the rainfall regime in the basin responds negatively in relation to El Niño and positive IOD rather than during La Niña and negative IOD. This entails that rainfall in the basin is related to Southern African rainfall, where low rainfall is displayed during El Niño. La Niña has been presented as the period when rainfall and discharge increases in the basin.

## 5.1 Recommendations for further studies

The study has demonstrated diverse results on the role that large forces modulate in the Pacific and Indian Oceans on Climate Variability. The present study would recommend the following for further studies:

- The studies related to the impact of global circulations seem to be different in each country; further studies should target local areas.
- Yet again, studies on the impact of the Indian Ocean Dipole on Climate and Hydrological response remain insufficient.
- Studies should look at the periodicities of IOD in relation to hydrometeorological parameters for modelling and prediction.
- ENSO/IOD influence on water availability should be studied at a local scale since its impact is not the same.

#### REFERENCES

- Asenahabi, B. M. (2019). Basics of research design: A guide to selecting appropriate research design. *International Journal of Contemporary Applied Researches*, 6(5), 76-89.
- Amirudin, A. A., Salimun, E., Tangang, F., Juneng, L., & Zuhairi, M. (2020).

  Differential influences of teleconnections from the Indian and Pacific oceans on rainfall variability in Southeast Asia. Atmosphere, 11(9), 13–15.

  https://doi.org/10.3390/ATMOS11090886
- Buishand, T.A. (1982). Some Methods for Testing the Homogeneity of Rainfall Records. J. Hydrol 58, 11-27
- Casimiro, W.S.L., Felipe, O., Silvestre, and E., Bourrel, L. (2013). ENSO impact on Hydrology in Peru. Adv.Geosci. 33, 33-39, 2013.Doi:10.5194/adgeo-33-33-2013.
- Chandimala, J., and Zubair, L. (2007). Predictability of Stream flow and rainfall based ENSO for water resources management in Sri Lanka. Journal of Hydrology.

  Available at <a href="https://www.elsevier.com/locate/jhydrol">www.elsevier.com/locate/jhydrol</a>
- Chaoka, R. T., Alemaw, B. F., Molwalelfhe, L., & Moreomongwe, O. M. (2006).

  Investigating the causes of water-well failure in the Gaotlhobogwe wellfield in southeast Botswana. *Journal of Applied Sciences and Environmental Management*, 10(3), 59-65.
- Coscarelli, R., and Caloiero, T. (2012). Analysis of daily and monthly rainfall

  Concentration in Southern Italy-Calabria region, J. Hydrol.

  DOI:10.1016/j.hydrol.2011.11.047
- Costa, A.C., and Soares, A. (2009). Homogenisation of climate Data: Review and New

- Perspectives Using Geostatistics. Math Geosci (2009) 41: 291-305. DOI 10.1007/s11004-008-9202-3.
- Fauchereau, N., Trzaska, S., Rouault, M., and Richard, Y. (2003). Rainfall variability and Changes in Southern Africa during the 20<sup>th</sup> Century in the global warming context, Nat. Hazards, 29,139-154, DOI: 10.1023/A: 1023630924100.
- Grubbs, F.E. (1969). Procedures for detecting outlying observations in Samples,

  Techno metrics, 11(1), 1-21
- Gabremicael, T.G., Mohammed, Y. A., Zaag, P.V., and Hagos, E.Y. (2017). Temporal and Spatial changes of rainfall and streamflow in the upper and Tekeze-Atbara river basin, Ethiopia. Hydrol. Earth Syst.Sci., 21, 2127-2142, 2017.
- Gemechu, T., Wakbulcho, G., Rao, G.N., and Adamu, T. (2015). the current and future

  Trend of Rainfall and its variability in Adami-Tulu Jido-Kombolcha Woreda,
- Central Rift Valley of Ethiopia. Journal of Environmental and Earth Science.ISSN 2225-0948(Online) Vol 5, No22, 2015.
- Goddard, L., and Graham, N.E. (1999). The Importance of the Indian Ocean for Simulating rainfall anomalies over eastern and southern Africa Journal of Geophysical Research 104: 19 099-19 116
- Gobena, A.K., and Gan., T.Y. (2006). Low-Frequency Variability in South-western

  Canadian Stream flow: Links with Large-Scale Climate Anomalies.

  International Journal of Climatology. 26: 1843-1869.DOI:10.1002/joc.1336
- Gyamfi, C., Ndambuki, J. M., and Salim, R.W. (2016). A Historical Analysis of
   Rainfall Trend in the Olifants Basin in South Africa. Vol 5. No 1.
   Doi: 10.5539/esr. v5n1p129. <a href="http://dx.doi.org/10.5539/esr.v5n1p129">http://dx.doi.org/10.5539/esr.v5n1p129</a>. Canadian
   Center of Science and Education
- Hoell, A., Funk, C., Zinke, J., and Harrison, L. (2017). Modulation of the southern

- Africa Precipitation response to the El Niño Southern Oscillation by the subtropical Indian Ocean dipole. Climate Dynamics, 48, 2529-2540. https://link.springer.com/article/10.1007/s00382-016-3220-6
- Hansel, S. Medeiros, D.M, Matschullat, J. Petta, R.A, and Silva, I. (2016). Assessing

  Homogeneity and Climate Variability of Temperature and Precipitation Series
  in the Capitals of North-Eastern Brazil. <a href="http://doi.org/10.3389/feart.2016.0029">http://doi.org/10.3389/feart.2016.0029</a>
- Hadgu, G., Tesfaye, K., Girma, M., and Kassa, B. (2013). Trend and Variability of rainfall in Tigray, Northern Ethiopia: Analysis of meteorological data and farmer's perception. University of Haramaya, College of Agriculture and Environmental Science.
- Hrudya, P. H., Varikoden, H., and Vishnu, R. (2021). A review on the Indian summer Monsoon rainfall, variability and its association with ENSO and IOD.
  Meteorology and Atmospheric Physics, 133, 1-14.
  https://link.springer.com/article/10.1007/s00703-020-00734-5
- Ibebuchi, C. C. (2023). Circulation Patterns Linked to the Positive Sub-Tropical Indian Ocean Dipole. Advances in Atmospheric Sciences, 40(1), 110–128. https://doi.org/10.1007/s00376-022-2017-2
- IPCC (2001) Climate Change. (2001). The Scientific Basis. In: J.T Houghton et al. (ed),
  Contribution of Working Group I to the Third Assessment Report of the
  Intergovernmental Panel on Climate Change Cambridge University Press,
  Cambridge, United Kingdom
- Isla, F.I., and Toldo, E. E. (2013). ENSO impacts on Atlantic watersheds of South

  America. Quaternary and Environmental Geosciences (2013)04(1-2):32-41

  Jury, M. R., & Mwafulirwa, N. D. (2002). Climate variability in Malawi, part

  1: dry summers, statistical associations and predictability. *International Journal*

- of Climatology: A Journal of the Royal Meteorological Society, 22(11), 1289-1302.
- Jiang, Y., Zhou, L., Roundy, P. E., Hua, W., & Raghavendra, A. (2021). Increasing

  Influence of Indian Ocean Dipole on Precipitation Over Central Equatorial

  Africa. *Geophysical Research Letters*, 48(8), 1–11.

  https://doi.org/10.1029/2020GL092370
- Jury, M.R. (2013). Climate Trends in Southern Africa. S. Afr J Sci. 2013; 109(1/2),
  Art. #980, 11 pages. http://dx.doi.org/10.1590/sajs.2013/980
- Kane, R.P. (2009). Periodicities, ENSO effects and trends of some South African rainfall Series: an update. *South African Journal of Science* 105, May/June 2009
- Karmeshu, N. (2012). Trend detection in annual temperature and precipitation using the Mann Kendall Test-A case study to Assess climate change on select states in the North-eastern United states. http://repository.upenn.

  Edu/mes\_capstones/47
- Kambombe, O. C., Ngongondo, C., Eneya, L., Monjerezi, M., & Boyce, C. (2021).

  Spatio-temporal analysis of droughts in the Lake Chilwa Basin, Malawi.

  https://doi.org/10.21203/rs.3.rs-272000/v1
- Kizza, M., Rhode A., Xu, Y.C., and Ntale, H.K. (2009). Temporal rainfall

  Variability in the Lake Victoria Basin East Africa during the twentieth centuary. *Theory Application Climatology* 98:119-135
- Kurniadi, A., Weller, E., Min, S. K., and Seong, M. G. (2021). Independent ENSO and IOD impacts on rainfall extremes over Indonesia. *International Journal of Climatology*, 41(6), 3640-3656. https://doi.org/10.1002/joc.7040
- Kumbuyo, C.P., Yasuda, H., Kitamura, Y., and Shimizu, K. (2014). Fluctuation of Rainfall time series in Malawi: An Analysis of Selected areas, GEOFIZIKA

- Vol 13, DOI 10.15233/gfz.2014.31.1
- Kug, J. S., Vialard, J., Ham, Y. G., Yu, J. Y., and Lengaigne, M. (2020). ENSO Remote forcing: influence of climate variability outside the tropical Pacific. *El Niño Southern Oscillation in a Changing Climate*, 247-265. doi/abs/10.1002/9781119548164.ch11
- Kumambala, P.G. (2010). Sustainability of water resources development for Malawi with particular emphasis on North and Central Malawi PhD thesis. University of Glasgow. http://theses.gla.ac.uk/1801/
- Mason, S.J., and Tyson, P.D. (1992). The modulation of Sea Surface Temperature and Rainfall associations over Southern Africa with Solar activity and Quasi Biennial Oscillation. Journal of Geophysical Research 97:5847-53-56
- Mbano, D., Chinseu, J., Ngongondo, C., Sambo, E and Mul, M. (2009). Impacts of Rainfall and Forest Cover Change on runoff in Small Catchments: A case study of Mulunguzi and Namadzi catchment areas in Southern Malawi. *Malawi Journal of Science and Technology*.
- Manatsa, D., Chingombe, W., and Matarira, C.H. (2008). The Impact of the Positive

  Indian Ocean dipole on Zimbabwe droughts. *International Journal of Climatology. Wiley Inter Science*. DOI:10.1002/joc.1695
- Mann-Whitney-Pettit test: Pettit A.N. (1979). A non- parametric approach to the Change-Point problem. App. Statist, 28, no.2: 126-135.
- Marchant, R. Mumbi, C. Behera, S. and Yamagata, T. (2007). The Indian Ocean

  Dipole-the Unsung driver of Climate Variability in East Africa, *African Journal*of Ecology, 45, 4-16
- Neukom, R., Nash, D.J., Endfield, G.H., Grab, S.W., Grove, C.A., Kelso, C., Vogel, C.H., and Zinke, J. (2014). Mult-proxy summer and Winter Precipitation

- Reconstruction for Southern Africa over the last 200 years. Climate Dyn., 42, 2713-2726, doi:10.0007/s00382-013-1886-6.
- Nash, D. J., Pribyl, K., Endfield, G. H., Klein, J., and Adamson, G. C. (2018). Rainfall Variability over Malawi during the late 19th century. *International Journal of Climatology*, 38, e629-e642. <a href="https://doi.org/10.1002/joc.5396">https://doi.org/10.1002/joc.5396</a>
- Nicholson, S.E., and Chavula, G. (2013). A detailed Rainfall Climatology for Malawi, Southern Africa. DOI:10.1002/joc.3637
- Ngongondo, C., Zhou, Y., & Xu, C. Y. (2020). Multivariate framework for the assessment of key forcing to Lake Malawi level variations in non-stationary frequency analysis. *Environmental Monitoring and Assessment*, 192(9). https://doi.org/10.1007/s10661-020-08519-4
- Ngongondo, C., Xu, C.Y., Gottschalk, L., and Alemw, B. (2011). Evaluation

  Of spatial and temporal characteristics of rainfall in Malawi: A case of data

  Scarce region, Theory. *Applied Climatology*. DOI: 10.1007/s00704-011-0413-0
- Ngongondo, C., Xu,Y. C., Tallaksen, L.M., and Alemw, B. (2014). Observed and Simulated changes in the water balance components over Malawi, during 1971-2000, *Quaternary International journal*. homepage:www.elsevier.com/locate/quaint
- Ngongondo, C., Li, L., Gong, L., Xu, C., and Alemaw, B. (2013). Flood frequency

  Under changing climate in the upper Kafue River Basin, Southern Africa: large
  scale hydrological model application. Doi: 1007/s00477-013-0724-z.
- Nnawuike, N. (2016). Assessment of the Impact of El Niño Southern Oscillation events

- On Rainfall amount in South-Western Nigeria. *Journal of Physical Science and Environmental studies*. Vol 2 (2), pp23-29.
- Nsubuga, F.W.N., Olwoch, I.M., and Rautenbach, C.I. (2011). Climatic trends at Namulonge in Uganda. *Journal of Geography*. 1947-2009.jGeogrGeo/3:119-131
- Ogwang, B.A., Ongoma, V., Xing, L., and Ogou, F.K. (2015). Influence of Mascarene High and Indian Ocean Dipole on East African Extreme Weather events. ISSN 0354-8724(hardcopy)/ISSN1820-7138 (online).
- Ogwang, B., Ongoma, V., Z. W., Shilenje, Z., Ramotubeir, T., M., Letum, M., &
- Ngain, J. (2021). Influence of Indian Ocean dipole on rainfall variability and extremes over southern Africa. *Mausam*, 71(4), 637–648. https://doi.org/10.54302/mausam.v71i4.50
- Phillips, C.L., Parr, J.M., and Riskin, E.A. (2008). Signals Systems and Transforms, Fourth. New Jersey: Prentice-Hall, 2008.
- Pui, A., Sharma, A.P.A., Santos, A., and Westra, S. (2011). Impact of the El Niño-Southern Oscillation, Indian Ocean Dipole, and Southern Annular Mode on Daily to Subdaily Rainfall Characteristics in East Australia.
- Pauw K., Thurlow J., and Seventer, D. (2010). Droughts and Floods in Malawi

  Assessing the Economy Wide Effects-Discussion Paper 00692. Washington

  D.C., United States of America
- Pettitt, A.N. (1979). A non-parametric approach to the change-point detection.

  Applied Statistics. 28, 126-135.doi:10.2307/2346729
- Rahman, A.S., Haddad, K., Rahman, A. (2014). Identification of Outliers in Flood

- Frequency Analysis: Comparison of Original and Multiple Grubbs-Beck Test. International Journal of Environmental and Ecological Engineering. Vol. 8. No 12.
- Reason, C., and Jagadheesha, D. (2005). A model investigation of recent ENSO impacts

  Over Southern Africa. Meteor. Amos. Phys., 89, 181-205
- Roudier, P., Ducharne, A., and Feyen, L. (2014). Climate Change impacts on runoff in West Africa: a review. *Hydrology Earth Science Systems*, 18.2789-2801, 2014
- Rouault, M., Monyela, B., Kounge, R. A. I., Stella, A., Njouodo, N., and Dieppois, B. (2019). Ocean impact on southern African climate variability and water resources. *Pretoria: Water Research Commission*. https://www.documentation.ird.fr/hor/fdi:010082414
- Roy, I. (2017). Indian Summer Monsoon and El Niño Southern Oscillation in CMIP5

  Models: A few Areas of Agreement and Disagreement.
- Rashid, A. (2004). Impact of El Niño on Summer Monsoon Rainfall of Pakistan.

  Pakistan Journal of Climatology. Vol. 1.
- Sahu, N., Yamashiki, Y., Avatar, R., Singh, R.B., and Takara, K. (2012). Impact of ENSO on the Paranaiba Catchment, Brazil. No. 55 B, 2012.
- Salau, O.R., Fasuba, A., Aduloju, K.A., Adesakin, G.E., and Fatigun, A.T. (2015).
  Effects of Changes in ENSO on Seasonal Mean Temperature and Rainfall in
  Nigeria. Climate 2016, 4, 5; doi: 10.3390/cli4010005. Available at
  http://www.mdpi.com/journal/climate
- Salehizadeh, A.A., Benshams, A., Ramanian, M., and Khodagholi, M. (2015). A study on ENSO Phenomenon Relationship with Fasa's Precipitation, Fasa Iran. *Journal of Applied Ecology and Environmental Sciences*, 2015, Vol. 3, No. 6, 158-162

- Salau, O.R., Schneider, B., Park, W., Khon, W., and Latif, M. (2012). Modelling the ENSO Impact of orbitally induced mean state climate changes. Geophysics. Res. 2012, 117.CrossRef.
- Saji, N.H., Goswami, B.N., Vinayachndra, P.N., and Yamagata, T. (1999). A dipole mode in tropical Indian Ocean. Nature 401:360-363
- Sitienei, B.J., Juma, S.G., and Opere, E. (2017). On the use of regression Models to Predict Tea Crop Yield Responses to Climate Change: A case of Nandi County Kenya. Climate 2017, 5, and 54: doi: 10.3390/cli5030054
- Susilo, G.E., Yamamoto, K., Imai, Ishii, Y., Fukami, H., and Sekine, M. (2013). The effect of ENSO on rainfall characteristics in the tropical peatland areas of Central Kalimantan, Indonesia. Hydrological Sciences Journal, 58 (3), 539-548.
- Tadeyo, E., Chen, D., Ayugi, B., & Yao, C. (2020). Characterization of spatio-temporal trends and periodicity of precipitation over Malawi during 1979-2015. *Atmosphere*, 11(9), 1–17. https://doi.org/10.3390/ATMOS11090891
- Thulu, F. G. D., Katengeza, E. W., & Mkandawire, M. (2017). Rainfall Trends for El Niño Seasons over Malawi from 1970 to 2016 and its Impact on Crop Yield and Hydropower Generation. *International Journal of Scientific and Research Publications*, 7(12). https://doi.org/10.13140/RG.2.2.14341.19689
- Tencaliec, P., Favre, A.C., Prieur C., Mathevet, T. (2015). Reconstruction of missing daily streamflow data using dynamic regression models. Water Resources Research, American Geophysical Union, 2015, 51(12), pp.9447-9463.
- Tukey, J.W. (1977). Exploratory Data Analysis Addison Wesley.
- Vincent, K., Dougill, A.J., Mkwambisi, D.D., Cull, T., Stringer, L.C., and Chanika, D. (2014). Analysis of Existing Weather and Climate Information for Malawi. Kulima Integrated Development Solutions.

- Ward, J.P., Beets, W., Bouwer, L.M., Aerts, J.C., and Renssen, H. (2010). Sensitivity of River Discharge to El Niño Southern Oscillation (ENSO). Geophysical Research Letter
- World Bank. (2010). Social dimensions of climate change: equity and vulnerability in A warming world. Washington DC.
- World Bank. (2003). Malawi and Southern Africa: Climatic Variability and Economic Economic Performance
- World Bank. (2009). Malawi: Economic Vulnerability and Disaster Risk Assessment:

  Draft final report. Vol 1.
- Yamagata, T., Behera, S.K., Rao, S.K., Guan, Z., Ashok, K., Saji, H.N. (2003).

  Comments on the dipole, temperature gradients and tropical climate anomalies.

  Bulletin of the American Meteorological society
- Zhang, Q., Xu, C.Y., Jiang, T., Wu, Y. (2006). Possible influence of ENSO on annual Maximum streamflow of the Yangtze River, China. Journal of Hydrology (2007), 265-274
- Zhang, Q., Xu, C.Y., and Chen, Y.D. (2008). Spatial and temporal variability of extreme Precipitation during 1960-2005 in the Yangtse River Basin and Possible Association with large-scale circulation J. Hydrol., 353,215-227, DOI: 10.1016/j.jhdrol. 2007.11.023
- Zubair, L. (2001). El Niño Southern Oscillation influences on the Mahaweli Streamflow in Sri Lanka. International Journal of Climatology, 23:91-102

## **APPENDICES**

## **APPENDIX** A. Homogenisation tests

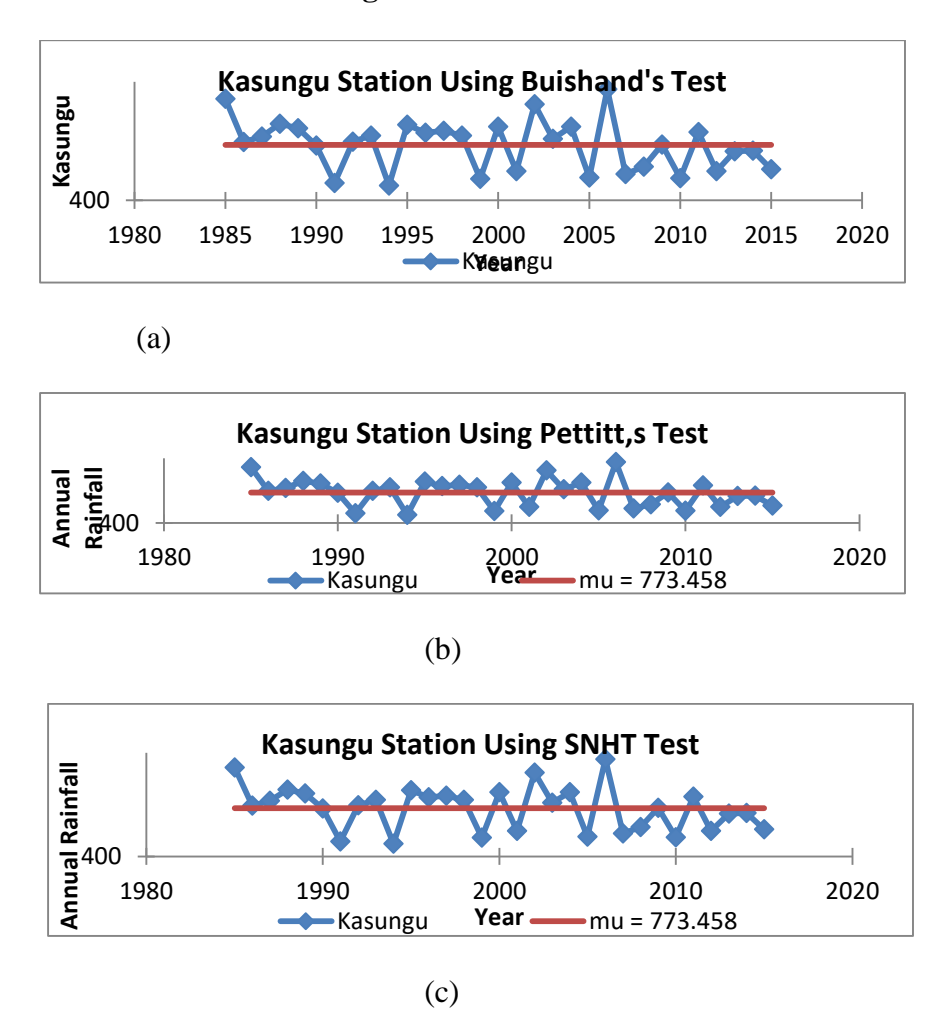
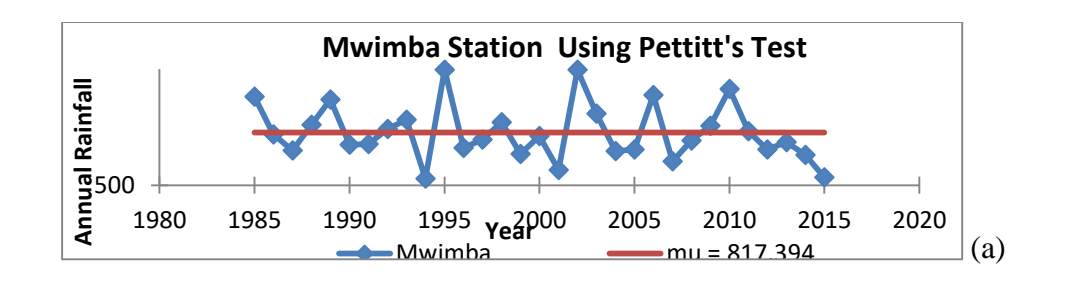
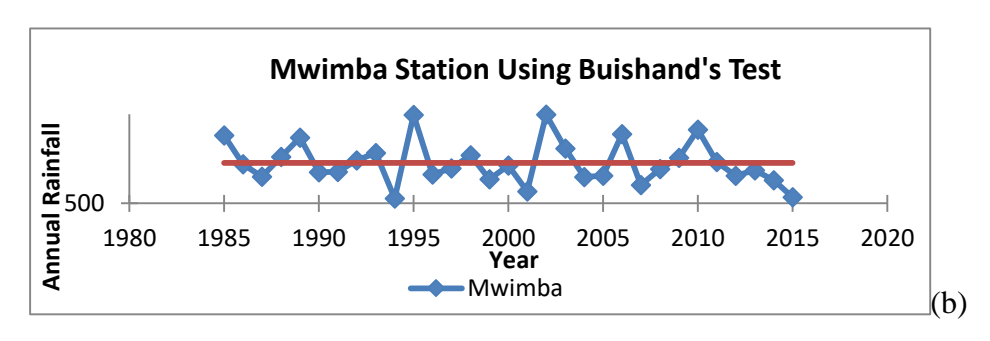


Figure 15 (a) Pettitt test (b) SNHT (c) Buishand Homogenisation tests graphs for Kasungu station





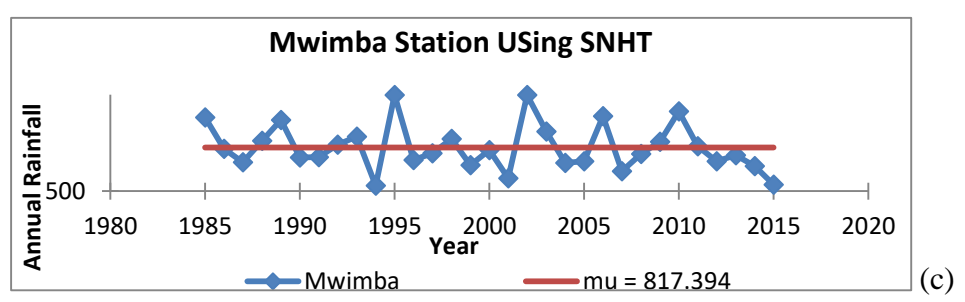


Figure 16 Homogeneity Test a, b, c and d

## **APPENDIX B Areal Mean Characteristics**

Table 16 Areal Mean Characteristics

Statistic	JAN	FEB	MAR	APR	MAY	JUN
Nbr. of	•					
observations	32	32	32	32	32	32
Minimum	396.250	404.925	325.350	72.125	0.000	0.000
Maximum	1152.825	992.900	1110.125	713.450	290.775	41.700
1st Quartile	581.100	586.456	521.781	205.231	16.975	0.188
Median	661.175	710.713	666.100	319.938	32.300	3.975
3rd Quartile	814.863	834.450	788.513	434.388	58.031	9.338
Mean	713.283	706.494	674.790	318.505	55.550	6.903
Variance (n-1)	34637.982	27712.318	45387.893	24234.718	4693.149	87.510

Standard
----------

deviation (n-1)	186.113	166.470	213.044	155.675	68.507	9.355
-----------------	---------	---------	---------	---------	--------	-------

JL AUG	CED				ANNUAL
IL AUG	CED				
	SEP	OCT	NOV	DEC	TOTALS
2 32	32	32	32	32	32
0.000	0.000	0.000	14.125	192.050	2291.975
3.600 17.625	105.575	82.500	477.450	970.450	4266.000
200 0.075	0.000	2.906	62.363	361.456	2780.256
075 1.213	2.038	15.788	105.225	494.113	3054.325
731 3.700	3.775	22.900	206.013	620.556	3538.975
168 3.180	7.238	17.509	141.730	495.874	3149.955
5.413 20.034	392.752	394.898	11432.762	33653.945	282814.776
819 4.476	19.818	19.872	106.924	183.450	531.803
0 3. 2 0 7 1 5.	32 000 0.000 .600 17.625 000 0.075 075 1.213 031 3.700 .68 3.180 .413 20.034	32 32 000 0.000 0.000 0.600 17.625 105.575 000 0.075 0.000 075 1.213 2.038 031 3.700 3.775 068 3.180 7.238 0.413 20.034 392.752	32 32 32 300 0.000 0.000 0.000 3600 17.625 105.575 82.500 300 0.075 0.000 2.906 375 1.213 2.038 15.788 31 3.700 3.775 22.900 368 3.180 7.238 17.509 392.752 394.898	32 32 32 32 300 0.000 0.000 0.000 14.125 3600 17.625 105.575 82.500 477.450 300 0.075 0.000 2.906 62.363 375 1.213 2.038 15.788 105.225 31 3.700 3.775 22.900 206.013 368 3.180 7.238 17.509 141.730 3413 20.034 392.752 394.898 11432.762	32 32 32 32 32 32 300 0.000 0.000 0.000 14.125 192.050 3600 17.625 105.575 82.500 477.450 970.450 300 0.075 0.000 2.906 62.363 361.456 375 1.213 2.038 15.788 105.225 494.113 31 3.700 3.775 22.900 206.013 620.556 3180 7.238 17.509 141.730 495.874 3413 20.034 392.752 394.898 11432.762 33653.945

# APPENDIX C. ANOVA for river discharge data

Figure 17 (a) ANOVA of S53 (b) Model Parameters (S53)

(a)

Source	Value	Standard	T	Pr >  t	Lower	bound	Upper bound
		error			(95%)		(95%)
Intercept	13.414	2.012	6.666	< 0.0001	9.438		17.390
Kwengwere	1.781	0.169	10.540	< 0.0001	1.447		2.115

Source	DF	Sum of squares	Mean squares	F	Pr > F		
Model	1	56137.878	56137.878	111.099	< 0.0001		
Error	150	75794.404	505.296				
<b>Corrected Total</b>	151	131932.282					
Computed against							
model Y=Mean(Y)							

(b)

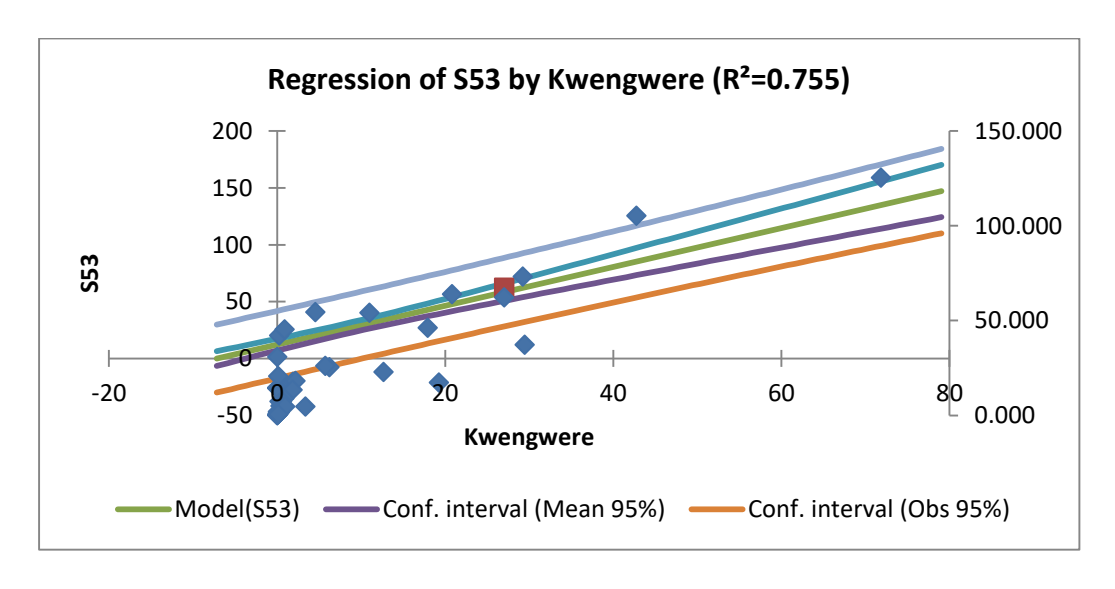


Figure 18 Regression graph of S53 by Kwengwere